CTEQ-TEA parton distribution functions now and in the future

Pavel Nadolsky

Southern Methodist University

CTEQ-TEA (Tung et al.) working group

Shanghai Jiao Tong University: J. Gao

Kennesaw State University: M. Guzzi

Michigan State University: J. Huston,
J. Pumplin, D. Stump, C. Schmidt, J. Winter,
C.-P. Yuan

Southern Methodist University: Tim Hobbs,
P. Nadolsky, B. T. Wang, K. P. Xie

Xinjiang University: S. Dulat, T.-J. Hou, I. Sitiwaldi

Frequently asked questions

1. **What is the meaning (definition) of my PDF?**
2. **Do I measure what I claim to be measuring?**
3. **How large are higher-order contributions?**
4. **How should the PDF uncertainties be estimated?**
5. **How much am I biased by my parametrization of PDFs?**
6. **Are there hidden PDF uncertainties?**

These questions are best understood for unpolarized collinear PDFs

$\Rightarrow$this talk and Tim Hobbs' talk

They must be addressed when trying to measure the nuclear, polarized, meson, TMD PDFs

Coordinated Theoretical Experimental study of QCD

Initiated around 1990 to stimulate interactions between

- Experimentalists and theorists, especially at the newly built Tevatron
- High-energy physics and hadronic physics communities

This is achieved by various initiatives:

- **Global analysis** *(the term coined by J. Morfin and Wu-Ki Tung)* constrains PDFs or other nonperturbative functions with data from diverse hadronic experiments

- **Workshops and summer schools**

- **Annual Wu-Ki Tung award** for junior researchers working on intersections of experiment and theory **[nomination deadline August 15 each year]**

…

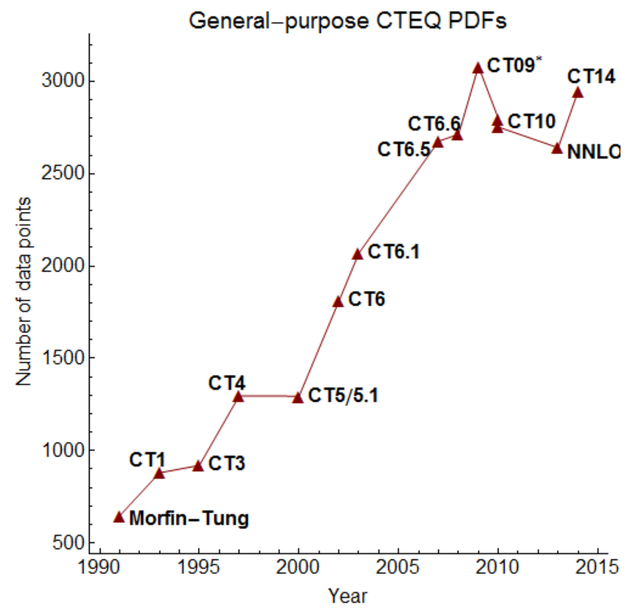

2018: new experiments (LHC, EIC, LHeC,…)! New objectives!

$$f_{a/h}(x,Q)$$

Unpolarized collinear parton distributions $f_{a/h}(x,Q)$ are associated with probabilities for finding a parton a with the "+" momentum xp^+ in a hadron h with the "+" momentum p^+ for $p^+ \to \infty$, at a resolution scale $Q > 1$ GeV

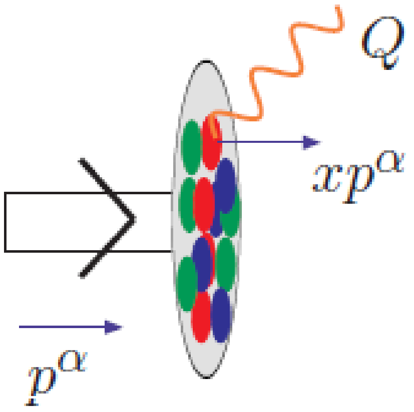

PDFs: key nonperturbative functions for LHC predictions

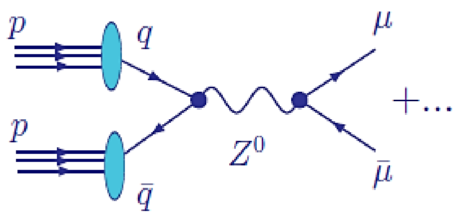

According to QCD factorization theorems, typical cross sections (e.g., for $p(k_1)p(k_2) \to \left[Z(q) \to \ell(k_3)\bar{\ell}(k_4)\right] X$) take the form

$$\sigma_{pp\to\ell\bar{\ell}X} = \sum_{a,b=q,\bar{q},g} \int_0^1 d\xi_1 \int_0^1 d\xi_2\, \widehat{\sigma}_{ab\to Z\to\ell\bar{\ell}}\left(\frac{x_1}{\xi_1}, \frac{x_2}{\xi_2}; \frac{Q}{\mu}\right) f_{a/p}(\xi_1,\mu) f_{b/p}(\xi_2,\mu) + \mathcal{O}\left(\Lambda^2_{QCD}/Q^2\right)$$

- $\widehat{\sigma}_{ab\to Z\to\ell\bar{\ell}}$ is the **hard-scattering cross section**
- $f_{a/p}(\xi,\mu)$ are the **PDFs**
- $Q^2 = (k_3+k_4)^2$, $x_{1,2} = (Q/\sqrt{s})\, e^{\pm y_V}$ — measurable quantities
- ξ_1, ξ_2 are partonic momentum fractions (integrated over)
- μ is a factorization scale (=renormalization scale from now on)

Parton distribution functions $f_{a/p}(x,Q)$...

... the best-known nonperturbative functions introduced in QCD

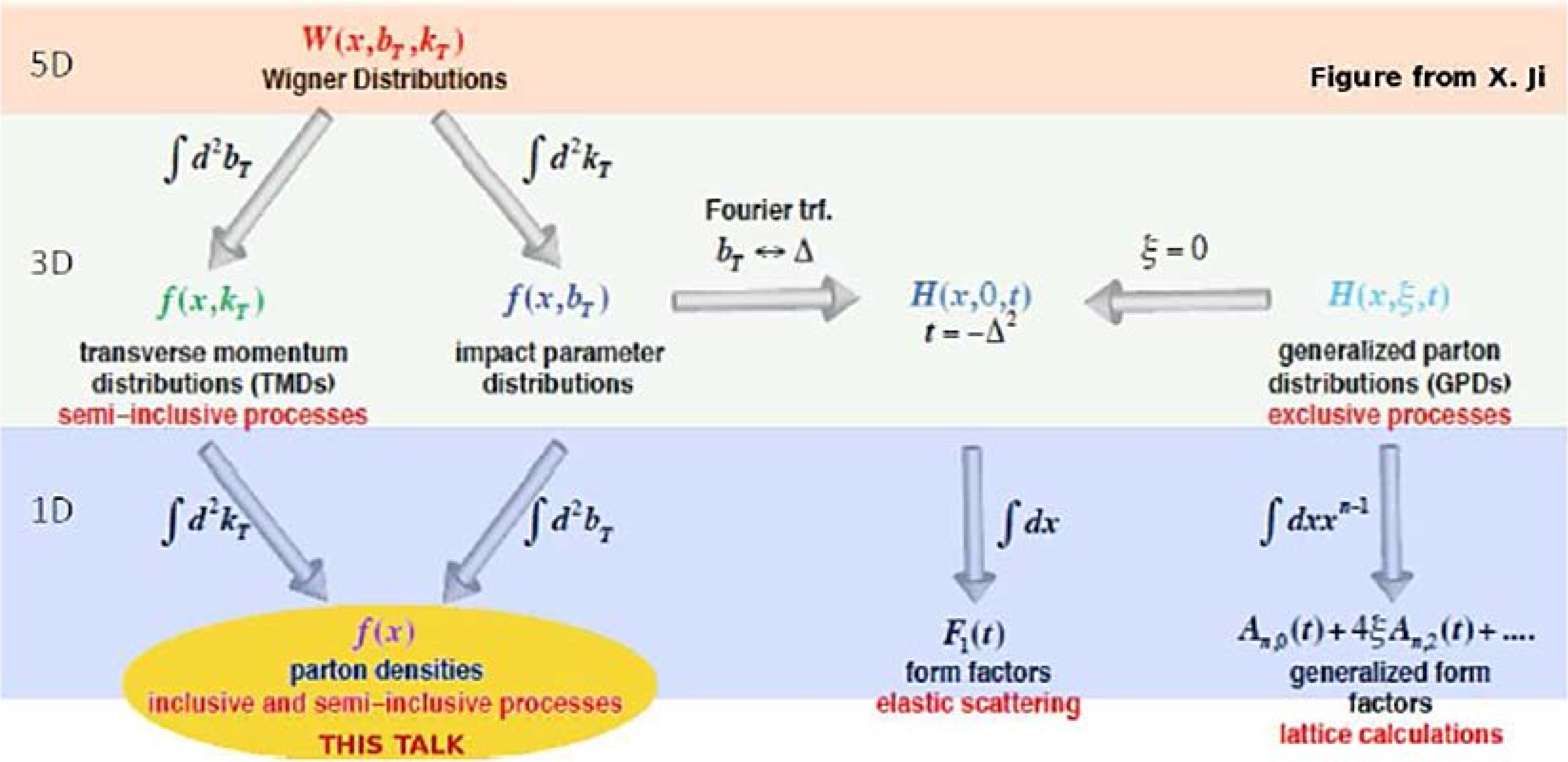

… can be obtained from Wigner distribution functions $W_{a/p}(x,p,s)$
… provide the baseline input for studies of polarized, nuclear, TMD, … PDFs

Perturbative QCD loop revolution

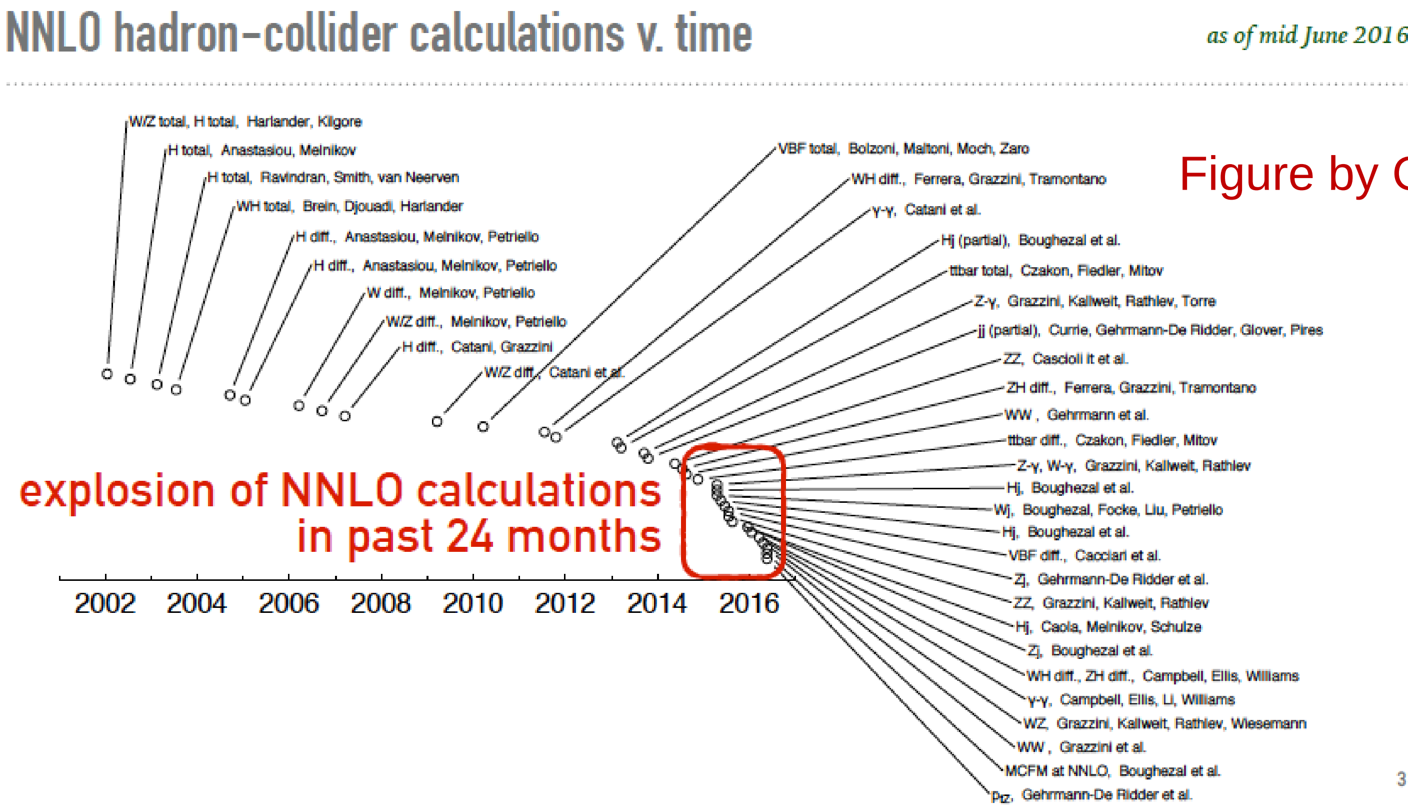

Figure by G. Salam

Since 2005, generalized unitarity and related methods dramatically advanced the computations of **perturbative** NLO/NNLO/N3LO hard cross sections $\hat{\sigma}$.

To make use of it, accuracy of PDFs $f_{a/p}(x,\mu)$ must keep up

Concepts of perturbative QCD at the LHC

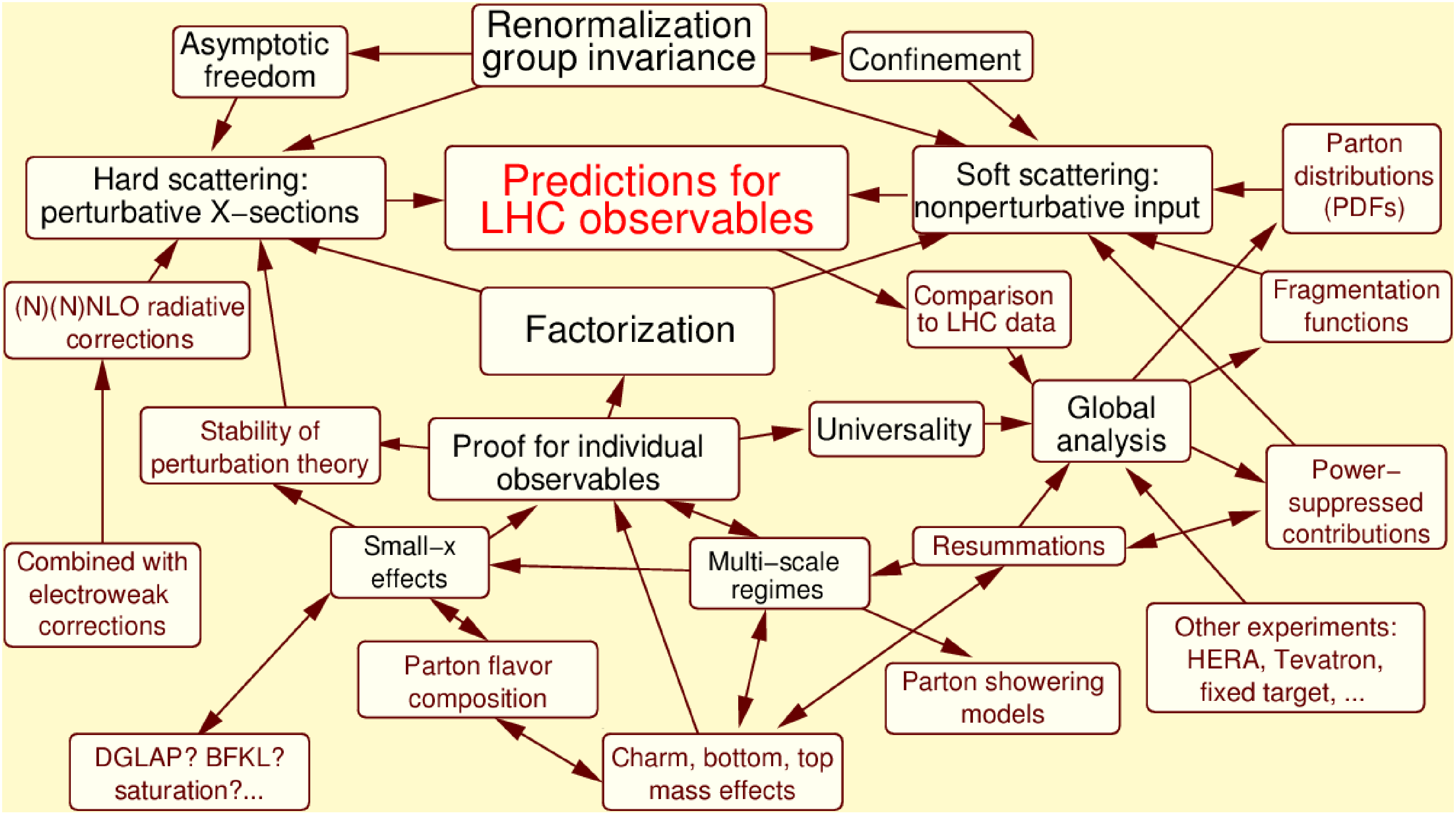

At the (N)NNLO accuracy level, multiple aspects affect the PDF behavior

Classes of PDFs

General-purpose

For (N)NLO calculations with $N_f \leq 5$ active quark flavors

From several groups:
ABMP'16
CTEQ-Jlab (CJ'2015)
HERA2.0
CT14 (→ 17p)
MMHT'14 (→ 16)
NNPDF3.1

Specialized

For instance, for CT14:
CT14 LO
CT14 $N_f = 3$, 4, 6
CT14 HERA2 **[arXiv:1609.07968]**
CT14 Intrinsic charm **[1707.00065]**
CT14 QCD+QED **[1509.02905]**
CT14 Monte-Carlo **[1607.06066]**

ATLAS & CMS exploratory

Combined **[1509.03865]**

PDF4LHC'15=CT14+MMHT'14+NNPDF3.0

CT14 Parton distributions

- 2015 major release on general-purpose PDFs, CT14 NNLO/NLO sets including alternative α_s series and $N_f = 3,4,6$ **[1506.07443]**

CT14 NNLO PDFs

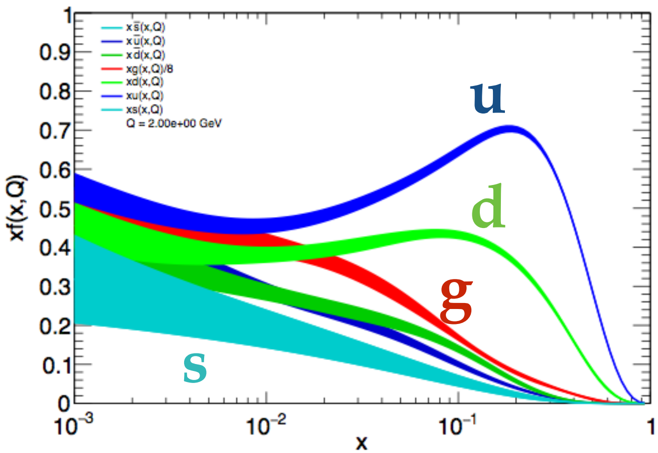

gluon-gluon luminosity

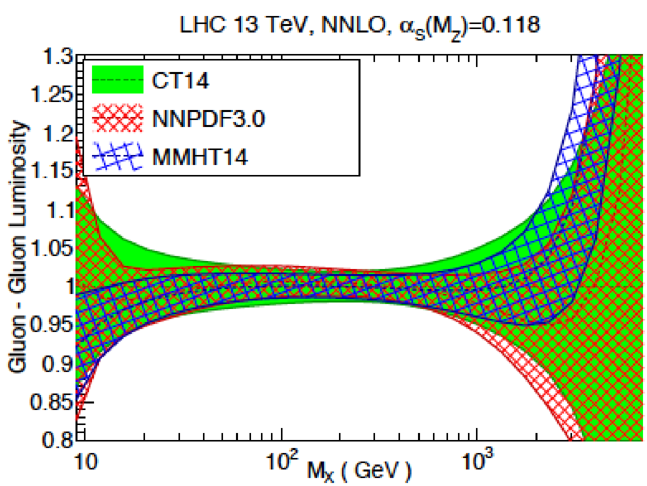

- combined HERA charm production, H1 FL data in NC DIS
- early LHC Run I data on W/Z charged lepton rapidity and asymmetry data;
- old D0 W-electron asymmetry data superseded by the new one with full luminosity;
- inclusive jet production from ATLAS and CMS

- more flexible parametrization for gluon, d/u at large-x, both d/u and dbar/ubar at small-x, 28 eigenvectors comparing to 25 for CT10

http://hep.pa.msu.edu/cteq/public/index.html

Toward a new generation of PDFs

[“CT17preliminary” PDFs]

Will the [high-luminosity] LHC fully constrain the PDFs?

2017-18: explicit and implicit advancements

All major groups rush toward implementing LHC data on **jet**, **W/Z,** $\boldsymbol{Z\ p_T\ t\bar{t}}$ production in the PDF analysis

- **ABMP'16** (arXiv:1701.05838) includes a large LHC W/Z data set, got closer to the other PDF sets ⇒ S. Moch

- The **NNPDF3.1** set has been released (arXiv:1706.00428), including a compatible subset of the new LHC data

- **CT1X** and **MMHT'XX** to be released within a few months, once compatibility of the new experiments is understood

However, reduction of the current PDF uncertainties is conditioned on understanding of (dis)agreement between the available data sets and improved control of theoretical and methodological uncertainties

Impressive Kinematic coverage

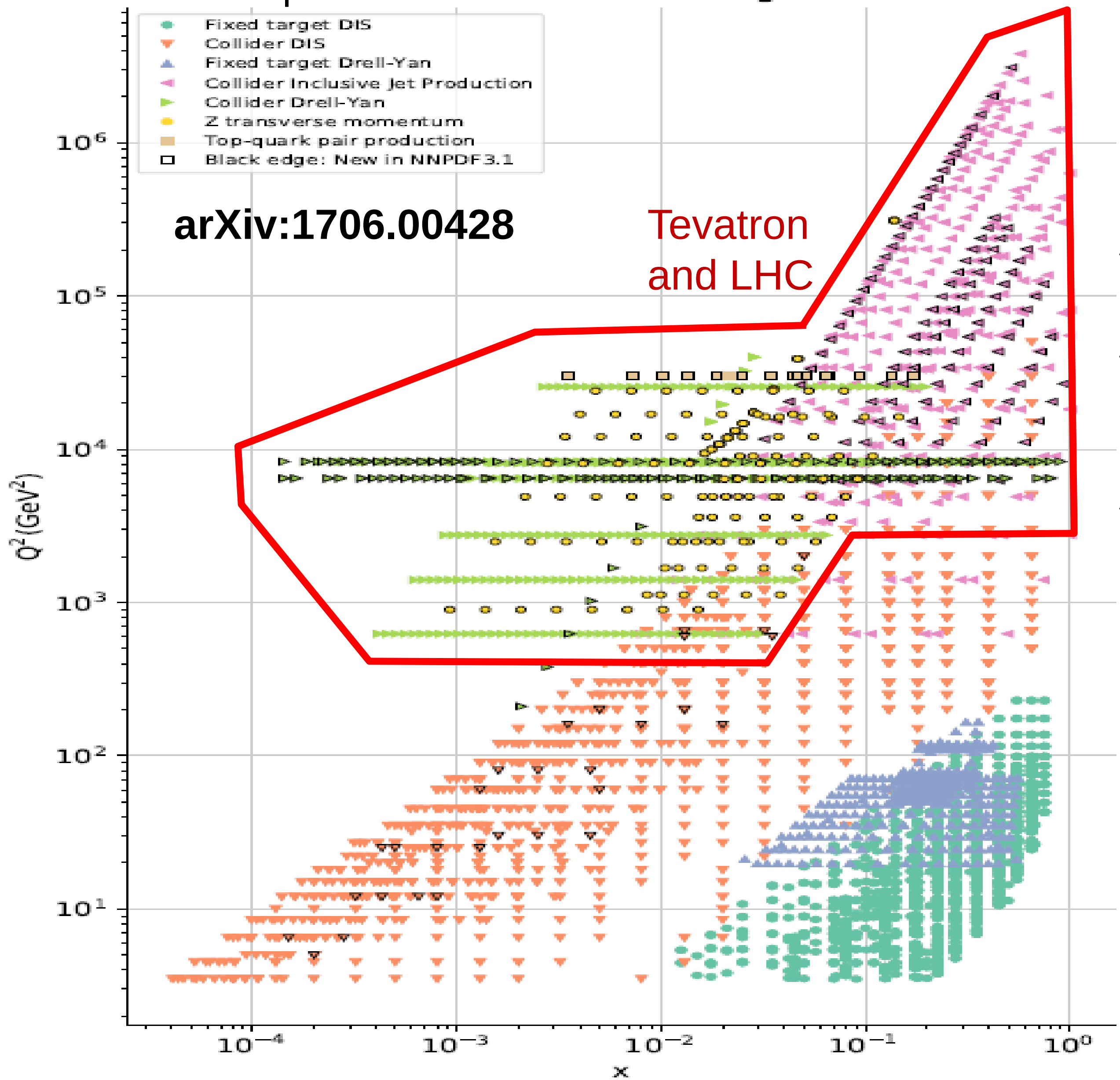

NNPDF3.1: the most **extensive** data set to date

3431 non-LHC (75%)+ **854 LHC data points (25%)**

A **subset** of available LHC data on $\ell\bar{\ell}$, jet, $\boldsymbol{Z\, p_T,\, t\bar{t}}$ production, analyzed at NNLO

$Z\ p_T,\ t\bar{t}$ moderately improve on NNPDF3.0 constraints on $g(x, Q)$ at x relevant for SM Higgs production

CT, MMHT also include D0 Run-2 jet production, get only slightly weaker constraints on $g(x, Q)$

CT14, MMHT14, NNPDF3.1 PDFs

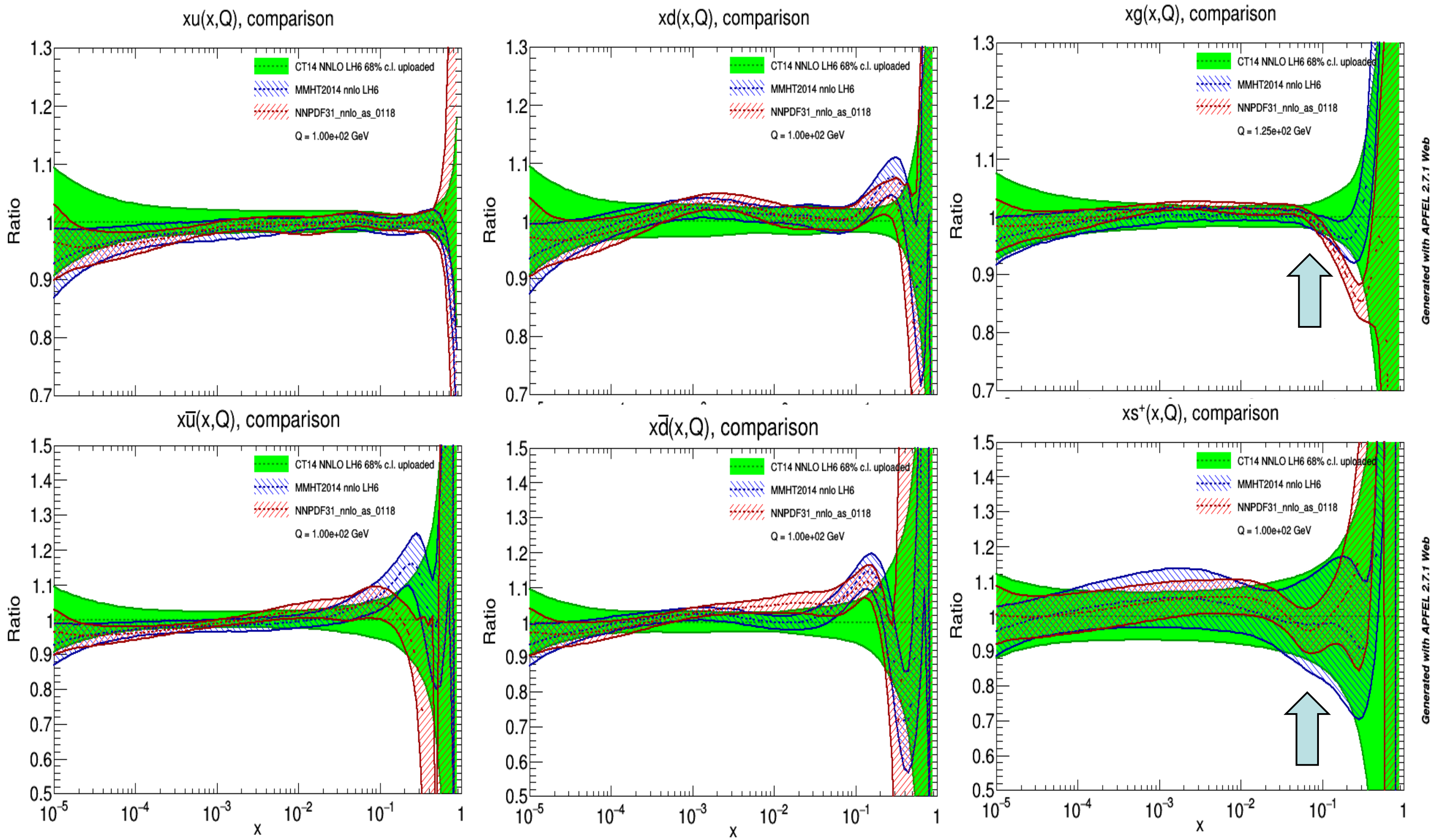

Central PDFs of 3 sets are compatible. The NNPDF3.1 uncertainty is moderately reduced on $g(x,Q)$ at $x > 0.05$, $s+\bar{s}$ at all x. The effect of the LHC data on the error bands does not exceed dependence on the definition of the PDF uncertainty (CT vs. MMHT vs. NNPDF).

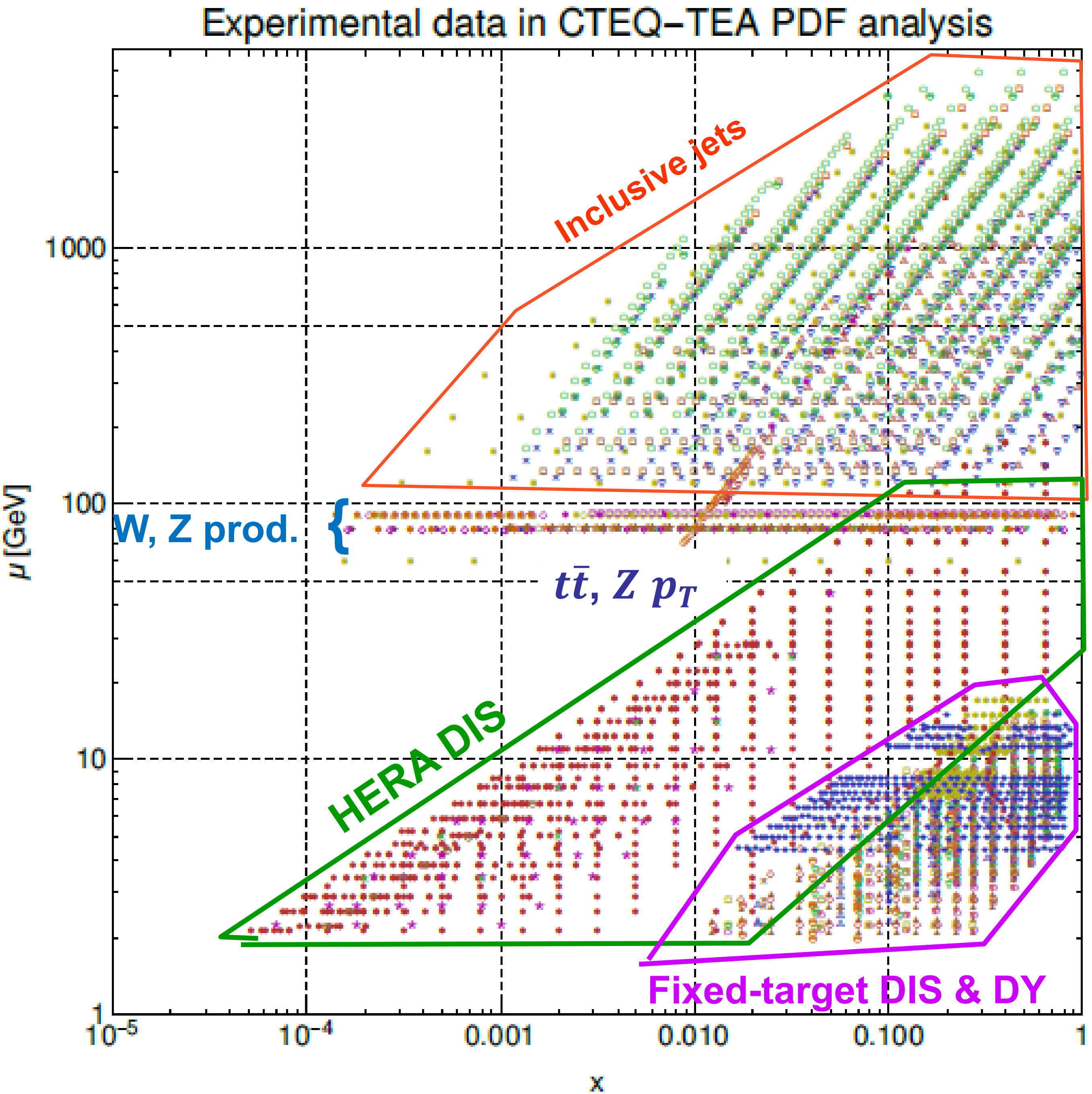

CT17pre analysis includes **new** LHC experiments on W/Z, high-p_T Z, jet, $t\bar{t}$ production

Experiments in the CT14 HERA2 fit

ID#	Experimental dataset		N_d
101	BCDMS F_2^p	[47]	337
102	BCDMS F_2^d	[48]	250
104	NMC F_2^d/F_2^p	[49]	123
108	CDHSW F_2^p	[50]	85
109	CDHSW F_3^p	[50]	96
110	CCFR F_2^p	[51]	69
111	CCFR xF_3^p	[52]	86
124	NuTeV $\nu\mu\mu$ SIDIS	[40]	38
125	NuTeV $\bar{\nu}\mu\mu$ SIDIS	[40]	33
126	CCFR $\nu\mu\mu$ SIDIS	[41]	40
127	CCFR $\bar{\nu}\mu\mu$ SIDIS	[41]	38
145	H1 σ_r^b (57.4 pb^{-1})	[53][54]	10
147	Combined HERA charm production (1.504 fb^{-1})	[39]	47
160	HERA1+2 Combined NC and CC DIS (1 fb^{-1})	[6]	1120
169	H1 F_L (121.6 pb^{-1})	[55]	9

ID#	Experimental dataset		N_d
201	E605 DY	[56]	119
203	E866 DY, $\sigma_{pd}/(2\sigma_{pp})$	[57]	15
204	E866 DY, $Q^3 d^2\sigma_{pp}/(dQdx_F)$	[58]	184
225	CDF Run-1 $A_e(\eta^e)$ (110 pb^{-1})	[59]	11
227	CDF Run-2 $A_e(\eta^e)$ (170 pb^{-1})	[60]	11
234	DØ Run-2 $A_\mu(\eta^\mu)$ (0.3 fb^{-1})	[61]	9
240	LHCb 7 TeV W/Z muon forward-η Xsec (35 pb^{-1})	[62]	14
241	LHCb 7 TeV W $A_\mu(\eta^\mu)$ (35 pb^{-1})	[62]	5
260	DØ Run-2 Z $d\sigma/dy_Z$ (0.4 fb^{-1})	[63]	28
266	CMS 7 TeV $A_\mu(\eta)$ (4.7 fb^{-1})	[64]	11
267	CMS 7 TeV $A_e(\eta)$ (0.840 fb^{-1})	[65]	11
268	ATLAS 7 TeV W/Z Xsec, $A_\mu(\eta)$ (35 pb^{-1})	[66]	41
281	DØ Run-2 $A_e(\eta)$ (9.7 fb^{-1})	[67]	13
504	CDF Run-2 incl. jet ($d^2\sigma/dp_T^j dy_j$) (1.13 fb^{-1})	[36]	72
514	DØ Run-2 incl. jet ($d^2\sigma/dp_T^j dy_j$) (0.7 fb^{-1})	[37]	110
535	ATLAS 7 TeV incl. jet ($d^2\sigma/dp_T^j dy_j$) (35 pb^{-1})	[68]	90
538	CMS 7 TeV incl. jet ($d^2\sigma/dp_T^j dy_j$) (5 fb^{-1})	[69]	133

New experiments in the CT17pre fit

1. LHCb 7 TeV Z/W muon rapidity 1505.07024
2. LHCb 8 TeV Z rapidity 1503.00963
3. CMS 8 TeV W lept. asymmetry 1603.01803
4. LHCb 8 TeV Z/W muon rapidity 1511.08039
5. ATLAS 7 TeV Z p_T 1512.02192
6. CMS incl. jet 7 TeV, R=0.7 1406.0324
7. ATLAS incl. jet at 7 TeV, R=0.6 1410.8857
8. CMS incl. jet at 8 TeV, R=0.7 1609.05331
9. ATLAS 8 TeV $t\bar{t}$ p_T 1511.04716
10. ATLAS 8 TeV $t\bar{t}$ $m_{t\bar{t}}$ 1511.04716
11. CMS 8 TeV $t\bar{t}$ $d^2\sigma/dp_{Tt}dy_t$ 1703.01630

N_d is the number of data points

CT17p: preliminary PDFs with new LHC data

Issues:

- Experimental, theoretical, and procedural **systematic** uncertainties dominate the PDF uncertainty in many cases
  - Tensions between some experimental data sets
  - Large QCD uncertainties in some kinematic regions (e.g., large y)

The CT17pre analysis examines how the PDFs depends on…

… settings of NNLO calculations

(SACOT-χ heavy-quark scheme, QCD scales, m_c, numerical codes,…)

… selection of experiments and kinematic cuts

For instance, $g(x,Q)$ at $x > 0.05$ is already constrained in CT14/MMHT14 by D0 Run-2 incl. jet data which is not in NNPDF3.1. Disagreements exist within available ATLAS/CMS experiments and between some LHC and non-LHC experiments

…the fitting procedure

Definition of PDF uncertainties

Parametrization forms

PDF error analysis (Hessian vs. Monte-Carlo)

…

How sensitive is an experiment to a PDF? Can we estimate it **before** doing the global fit?

Yes, using new statistical tools:

1. Generalized correlations (**sensitivities** S_f) comparing experimental and PDF uncertainties for fitted data points

PDFSense (1803.02777)
http://metapdf.hepforge.org/PDFSense

2. PDF reweighting
3. Hessian profiling

} ⇒ mcgen (1607.06066)
ePump (1806.07950)

Statistical methods to identify the PDF dependence

1. PDF-driven correlations with theory cross sections [**arXiv:0802.0007**]

If the **theory** cross section σ is sensitive to a given PDF f, the Hessian correlation $\cos\varphi$ is close to ± 1

Correlation between σ_W/σ_Z and f(x,Q=85 GeV)

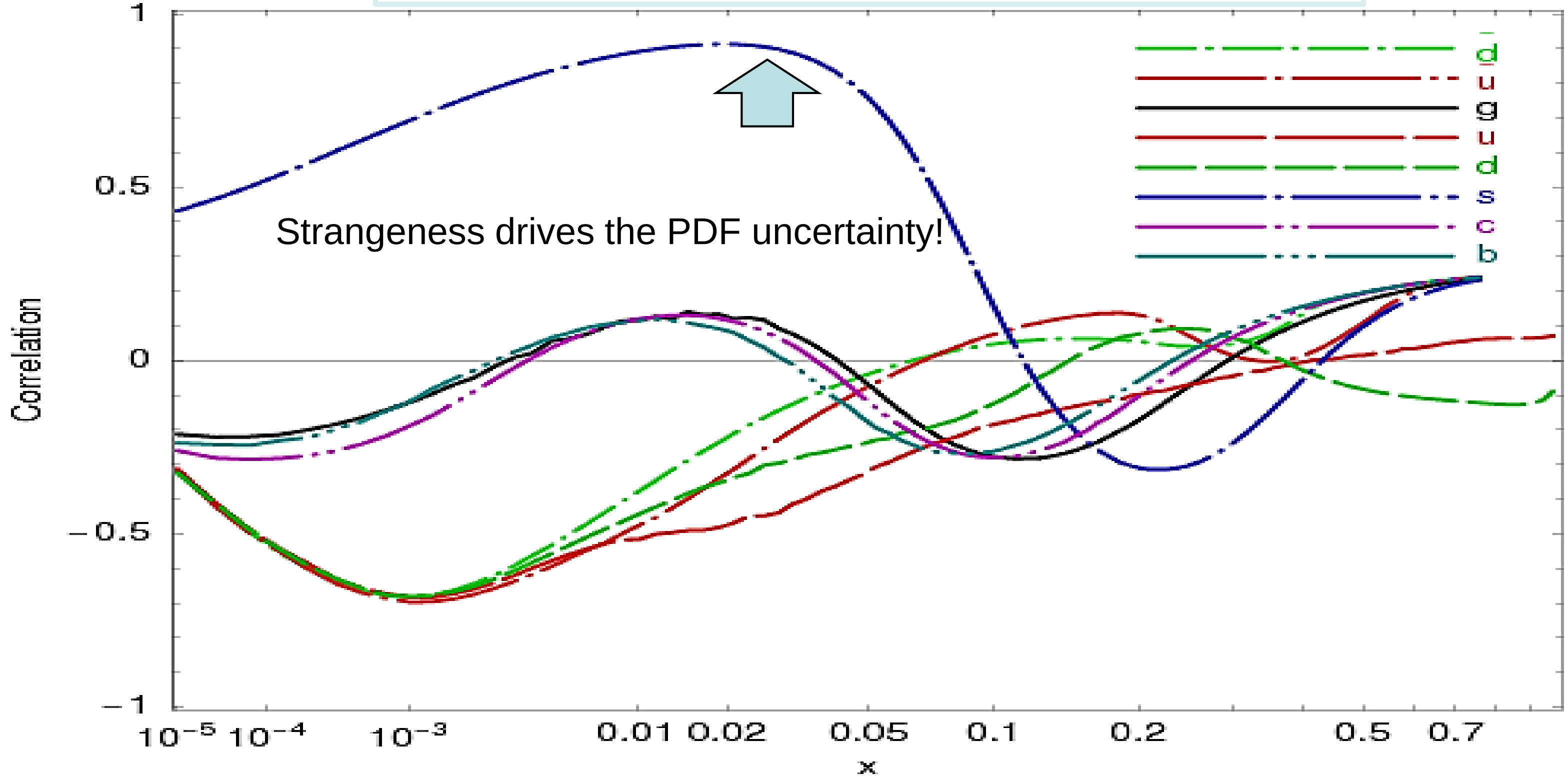

Before the fit

Statistical methods to identify the PDF dependence

2. Sensitivity of a data point
[B.W. Wang, T.J. Hobbs, et al., arXiv:1803.02777; **program PDFSense**]

If a **data point** is sensitive to a given PDF f, then the sensitivity $|S_f|$ of this data point to f is much larger than 0 [say, $|S_f| > 0.25$]. S_f is defined on the next slide.

Sensitivity to the PDF error on $\sigma(pp \to H^0 X)$ at 14 TeV

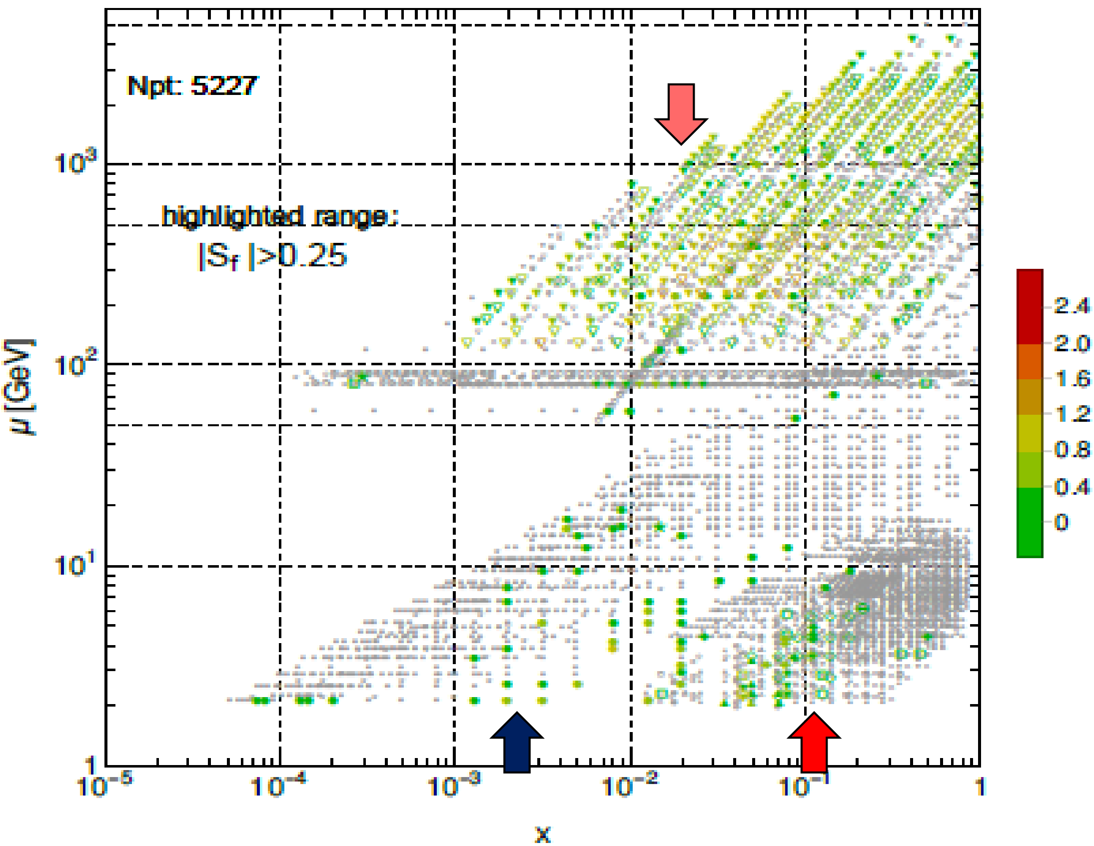

Before the fit

Correlation C_f and sensitivity S_f

The relation of data point i on the PDF dependence of f can be estimated by:

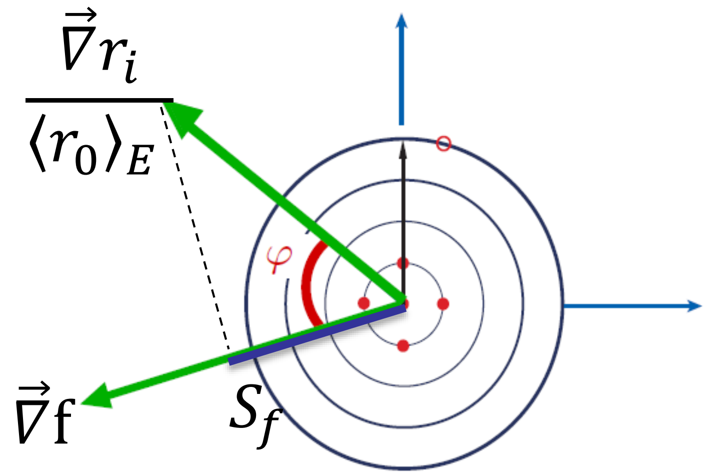

- $C_f \equiv \text{Corr}[\rho_i(\vec{a})), f(\vec{a})] = cos\varphi$

$\vec{\rho}_i \equiv \vec{\nabla} r_i / \langle r_0 \rangle_E$ -- gradient of r_i normalized to the r.m.s. average residual in expt E;

$$\left(\vec{\nabla} r_i\right)_k = \left(r_i(\vec{a}_k^{+}) - r_i(\vec{a}_k^{-})\right)/2$$

C_f is **independent** of the experimental and PDF uncertainties. In the figures, take $\left|C_f\right| \gtrsim 0.7$ to indicate a large correlation.

- $S_f \equiv |\vec{\rho}_i| cos\varphi = C_f \frac{\Delta r_i}{\langle r_0 \rangle_E}$ -- projection of $\vec{\rho}_i(\vec{a})$ on $\vec{\nabla} f$

S_f is proportional to $\cos\varphi$ and the ratio of the PDF uncertainty to the experimental uncertainty. We can sum $|S_f|$.
In the figures, take $\left|S_f\right| > 0.25$ to be significant.

Higgs boson production

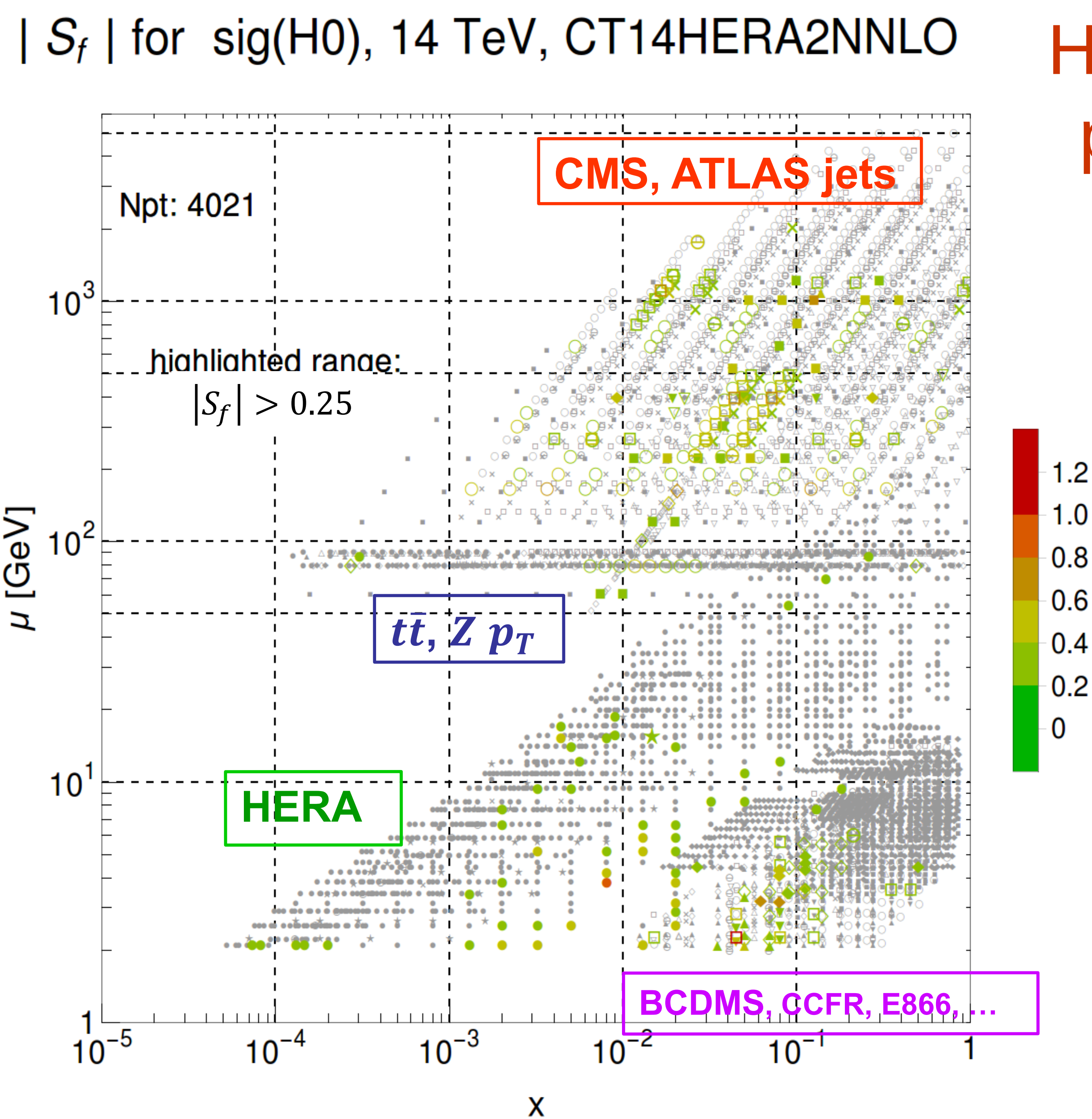

HERA DIS still has the dominant sensitivity!

CMS 8 TeV jets is the next expt. after HERA sensitive to $\sigma_H(14$ TeV); jet scale uncertainty dampens $|S_f|$ for jets

Good correlations C_f with some points in E866, BCDMS, CCFR, CMS WASY, $Z\ p_T$ and $t\bar{t}$ production; but not as many points with high $|S_f|$ in these processes

Gluon PDF before and after including the LHC data

[CT14HERA2 vs. CT17pre NNLO]

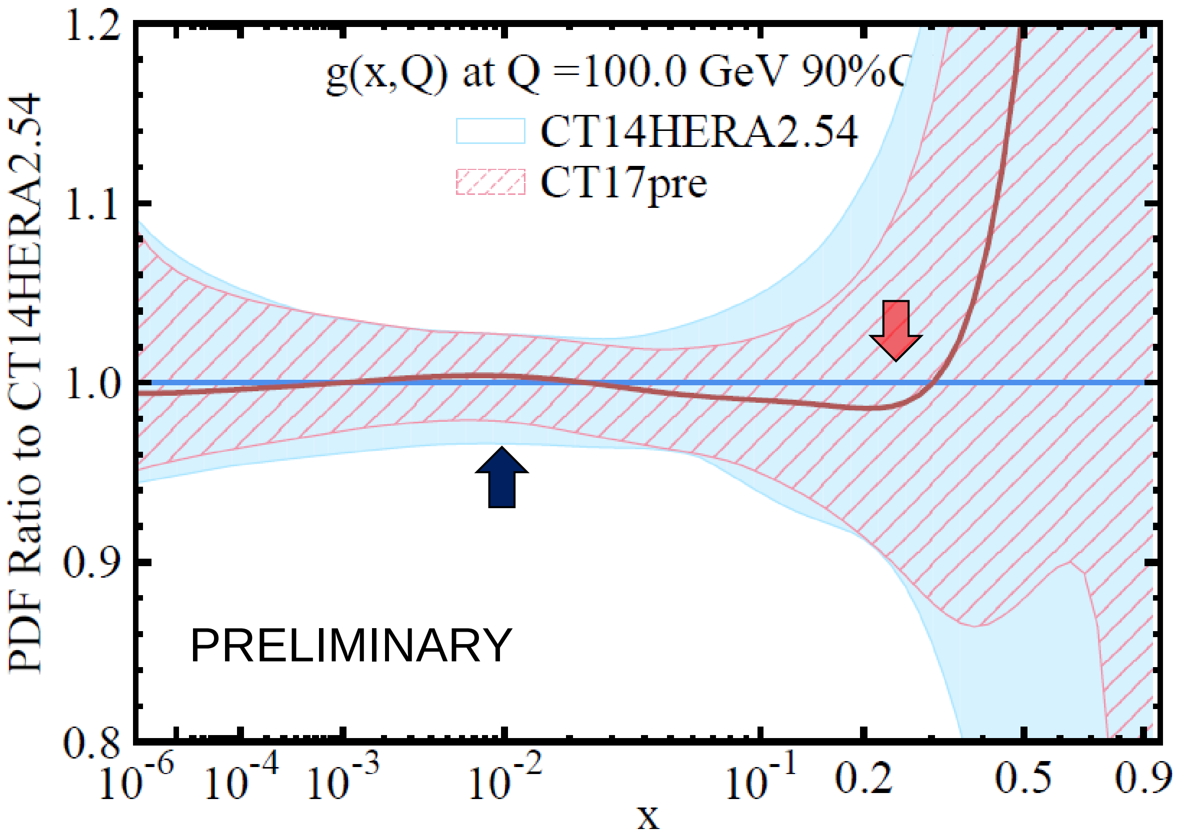

$x \approx 0.01$: $g(x,Q)$ mildly increases within the uncertainty

⇒ slightly larger Higgs production rates at 14 TeV

Minor reduction in the gluon PDF uncertainty

$0.05 \lesssim x \lesssim 0.3$: $g(x,Q)$ mildly decreases; lower gg luminosities for $M_X > 700$ GeV

After the fit

Which experiments constrain the gluon? $x = 0.01, Q = 125$ GeV [Higgs region]

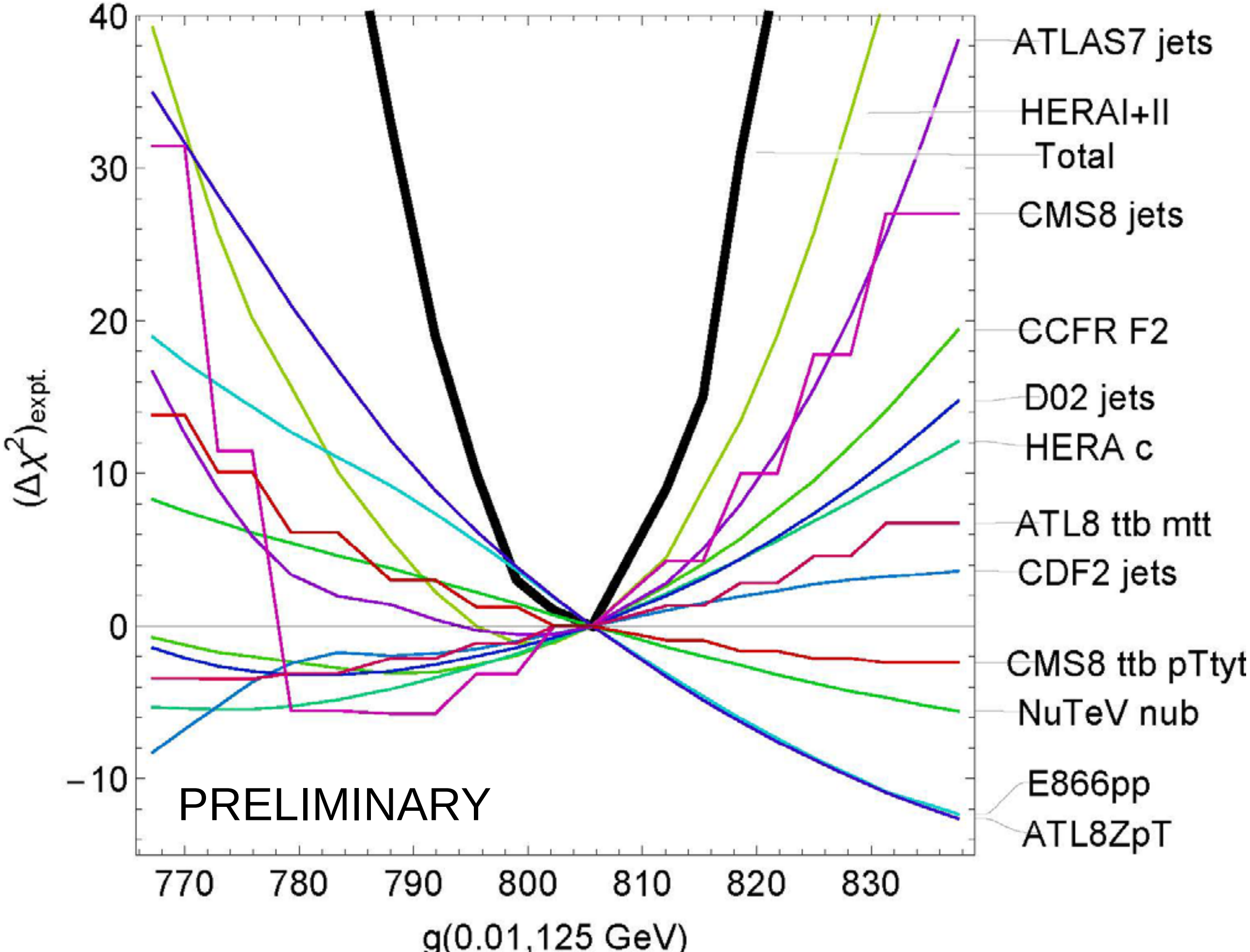

A Lagrange multiplier scan [Stump et al., hep-ph/0101151] of

$$\Delta\chi^2 = \chi^2(g) - \chi^2_{best-fit}$$

for all (black line) and individual (colored lines) experiments

Best-fit $g(0.01,125\text{GeV})$=806

After the fit

Which experiments constrain the gluon? $x = 0.01, Q = 125$ GeV [Higgs region]

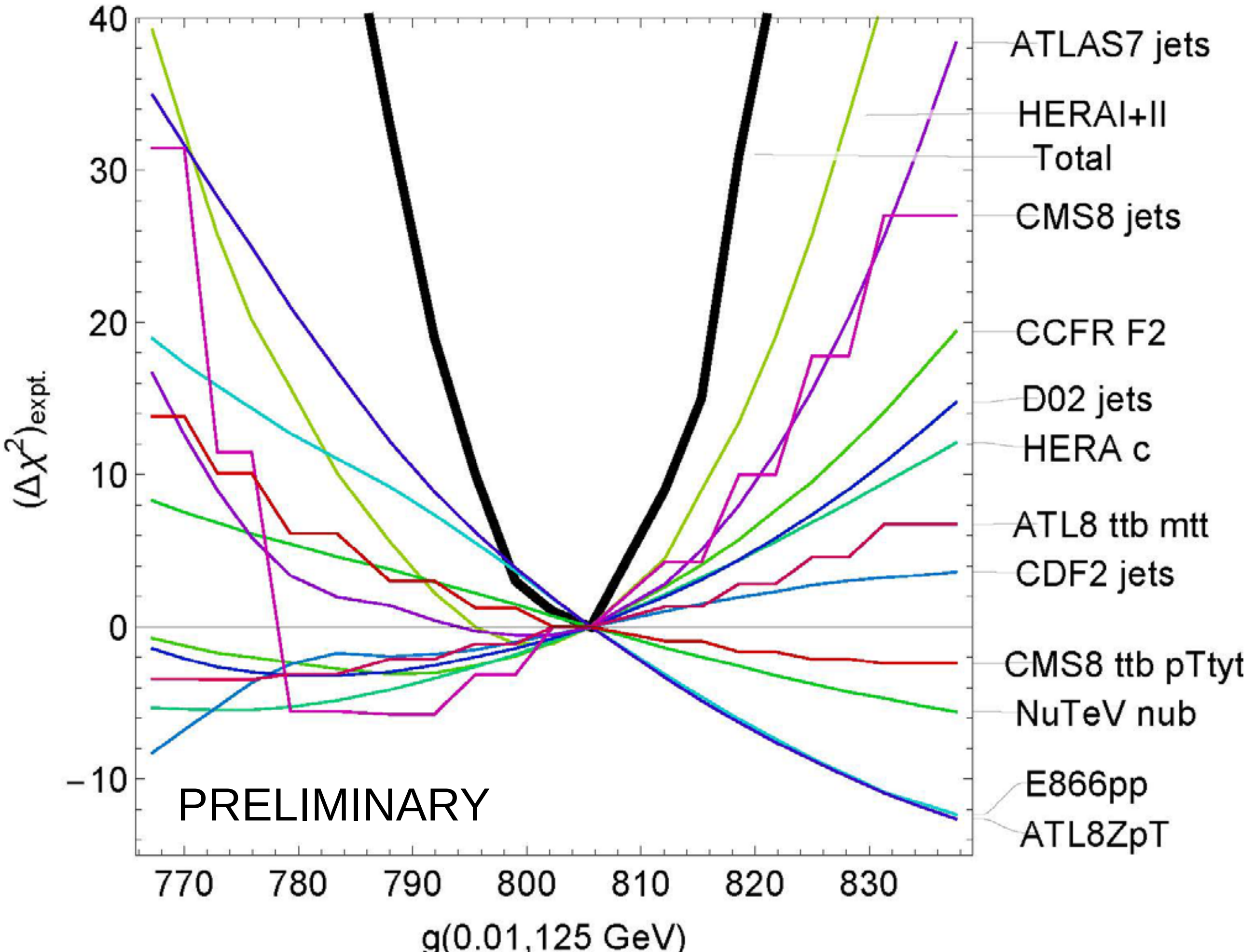

The LM scans broadly confirm S_f estimates

HERAI+II, ATLAS7 jets, CMS8 jets impose the tightest constraints; are in agreement

E866, ATLAS 8 Z p_T prefer higher gluon

After the fit

Which experiments constrain the gluon? $x = 0.3, Q = 125$ GeV

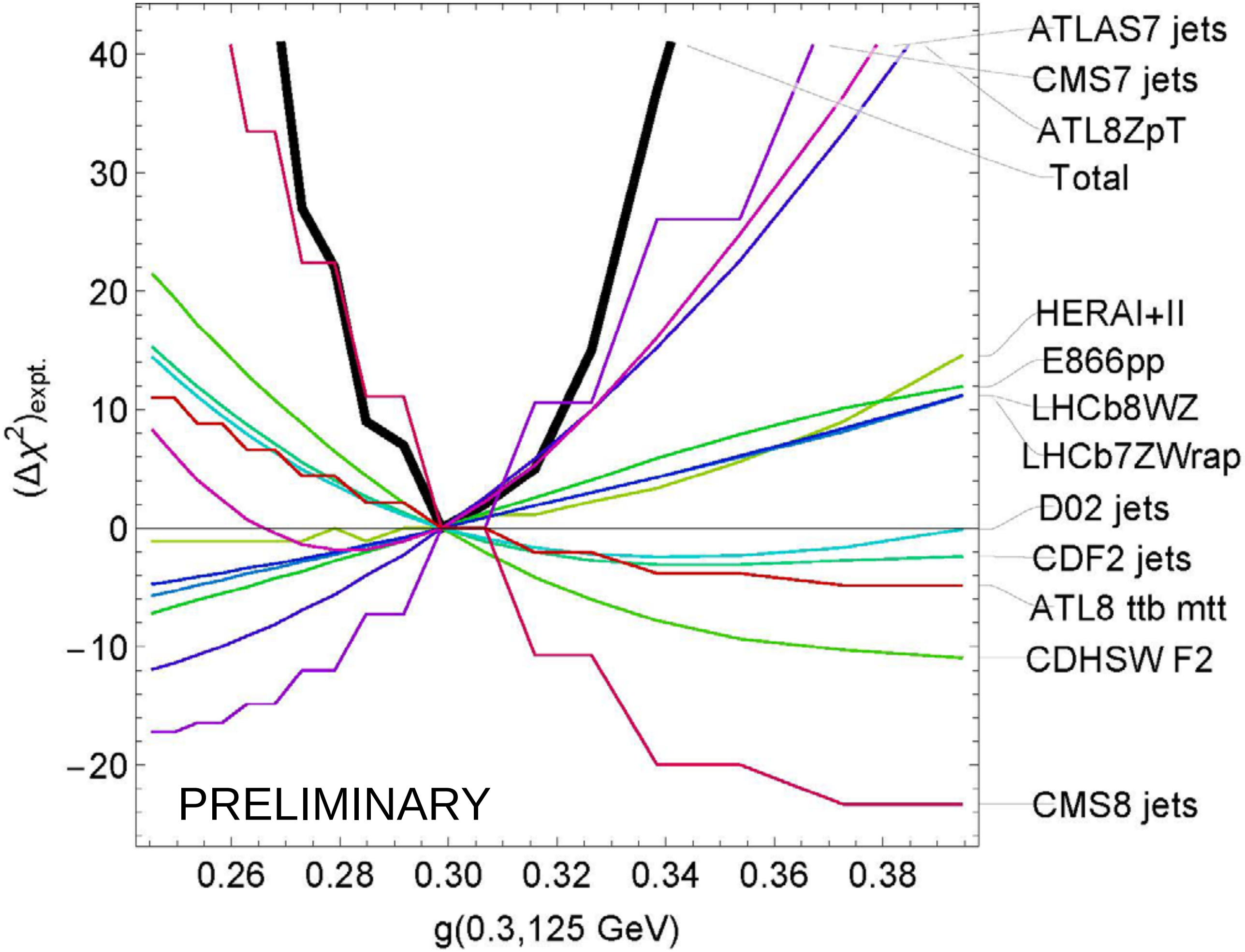

ATLAS 7 and CMS 7 TeV jets, ATLAS 8 Z p_T disagree with CMS8 jets

Weaker constraints from HERAI+II, E866, LHCb, Tevatron jets, CDHSW F2, $t\bar{t}$ production

After the fit

Preview of CT17pre
($\bar{u}$-PDF and $\bar{d}$-PDF)

PRELIMINARY

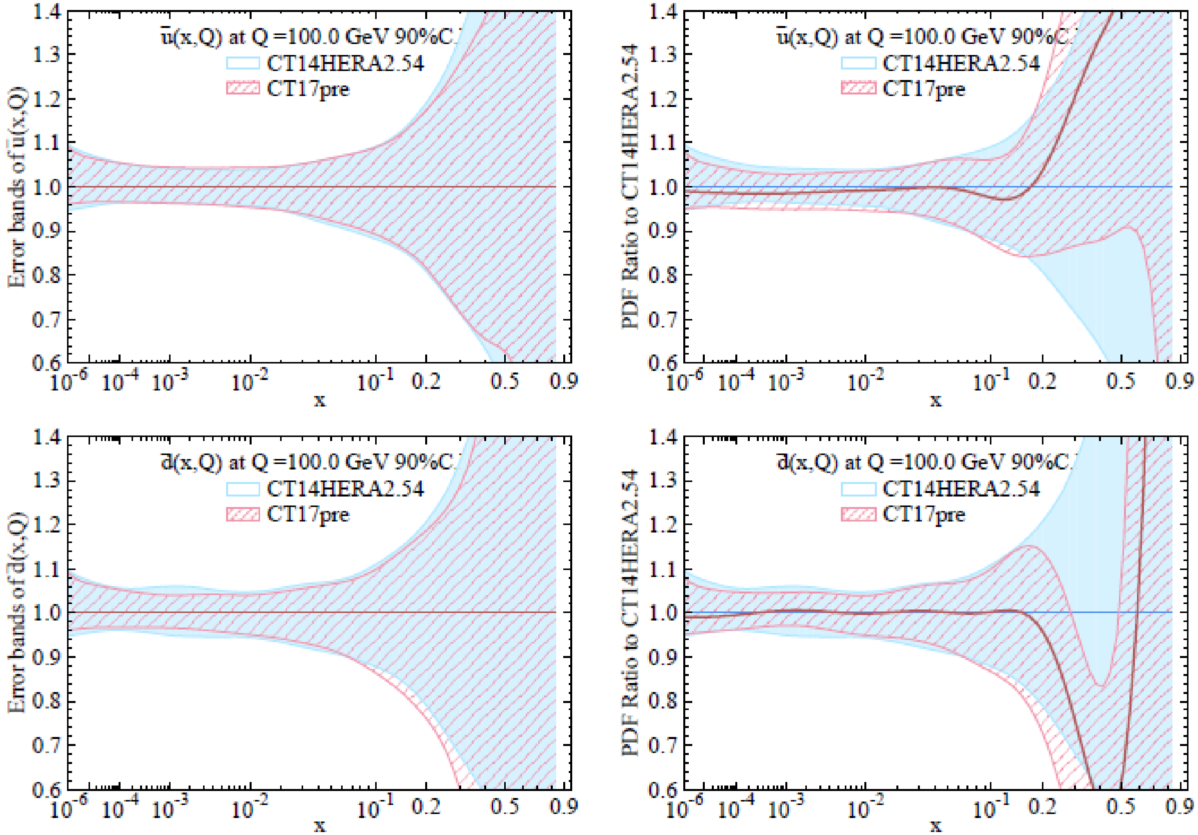

- Similarly, minor changes on $\bar{u}$ and $\bar{d}$ at small x region mainly come from LHCb W and Z rapidity data, at 7 and 8 TeV..
- The behavior of $\bar{u}$ and $\bar{d}$ as $x \to 1$ is parametrization form dependent.

Preview of CT17pre (u-PDF and d-PDF)

PRELIMINARY

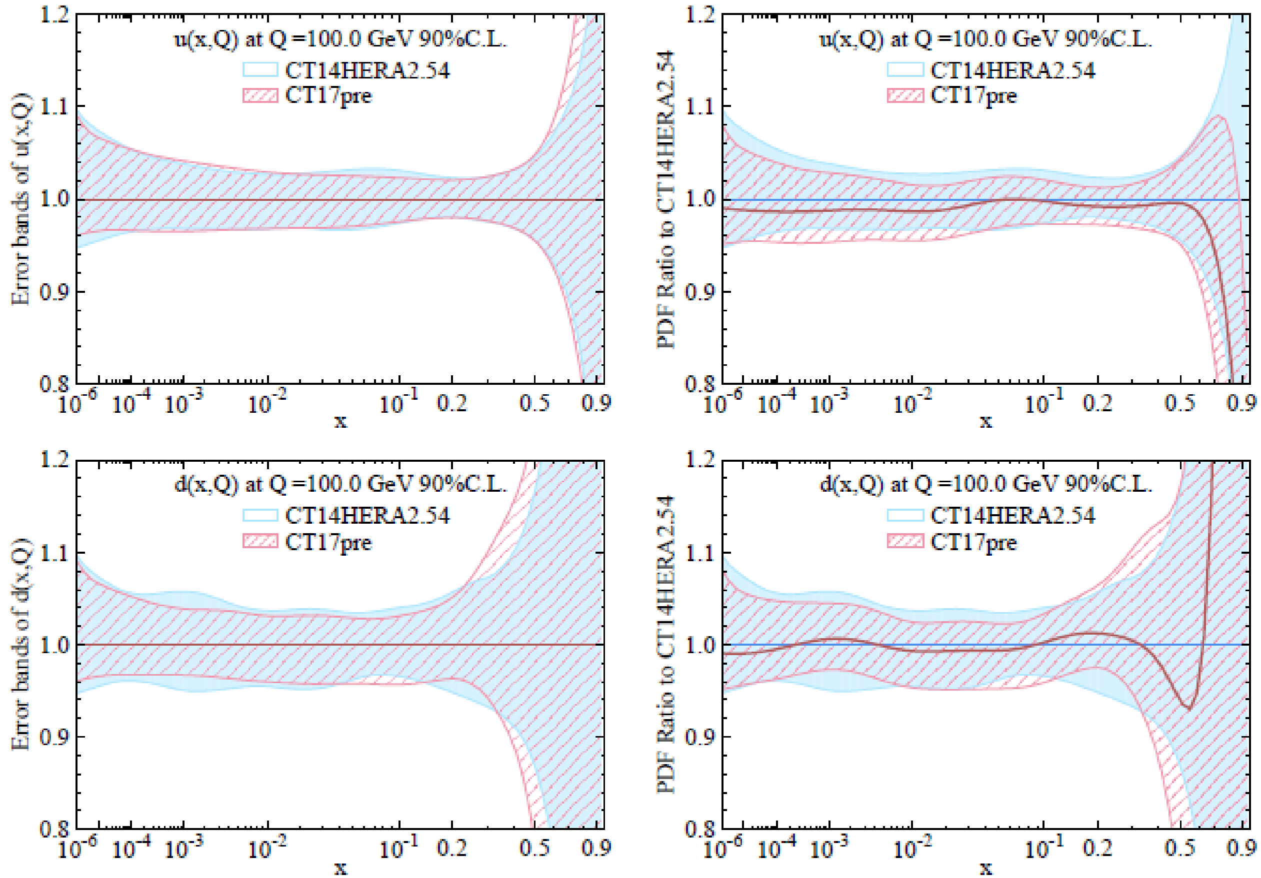

- Some changes on *u* and *d* at small x region and d around 0.2 mainly come from LHCb W and Z rapidity data, at 7 and 8 TeV.

Inconsistent conclusions in literature about strangeness preferred by the LHC data

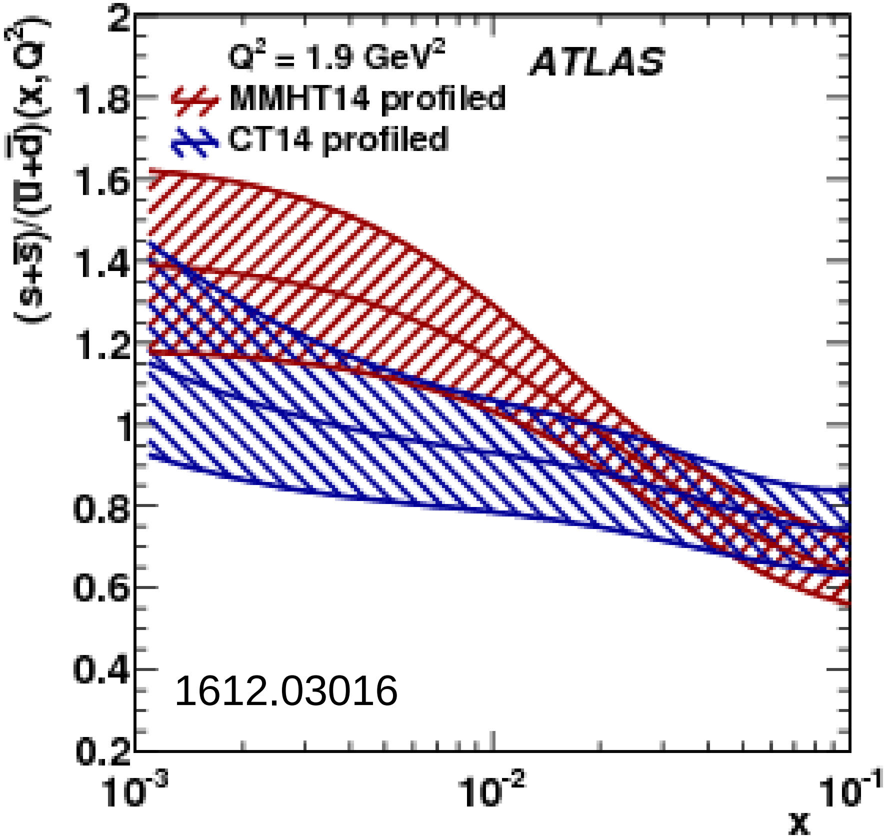

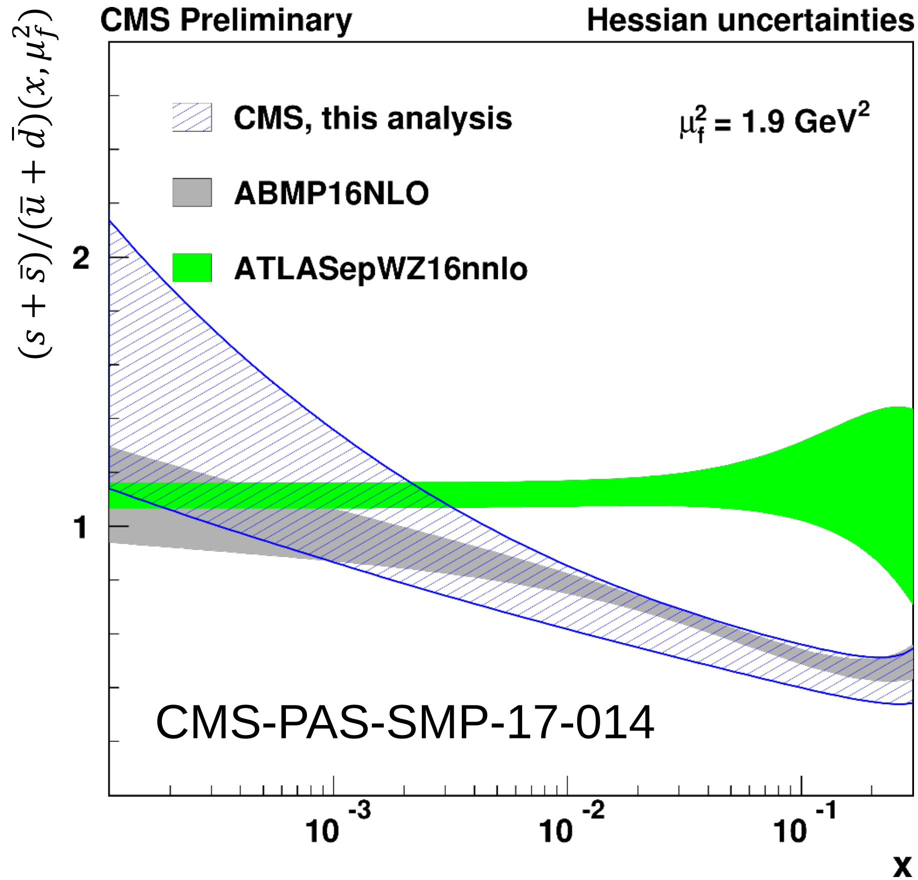

CT14 and MMHT14 NNLO PDFs profiled using ATLAS 7 TeV (4.6 fb^{-1}) $W^{\pm}$, Z xsecs prefer $s(x, 1.9\ GeV) \sim 1\ \ @\ x = 0.023$

CMS W,Z, CMS W+c (13 TeV) prefer smaller $s(x,\mu)$ than ATLAS for $x \gtrsim 10^{-3}$

Effect of LHC data on strangeness: the actual CT17pre fit

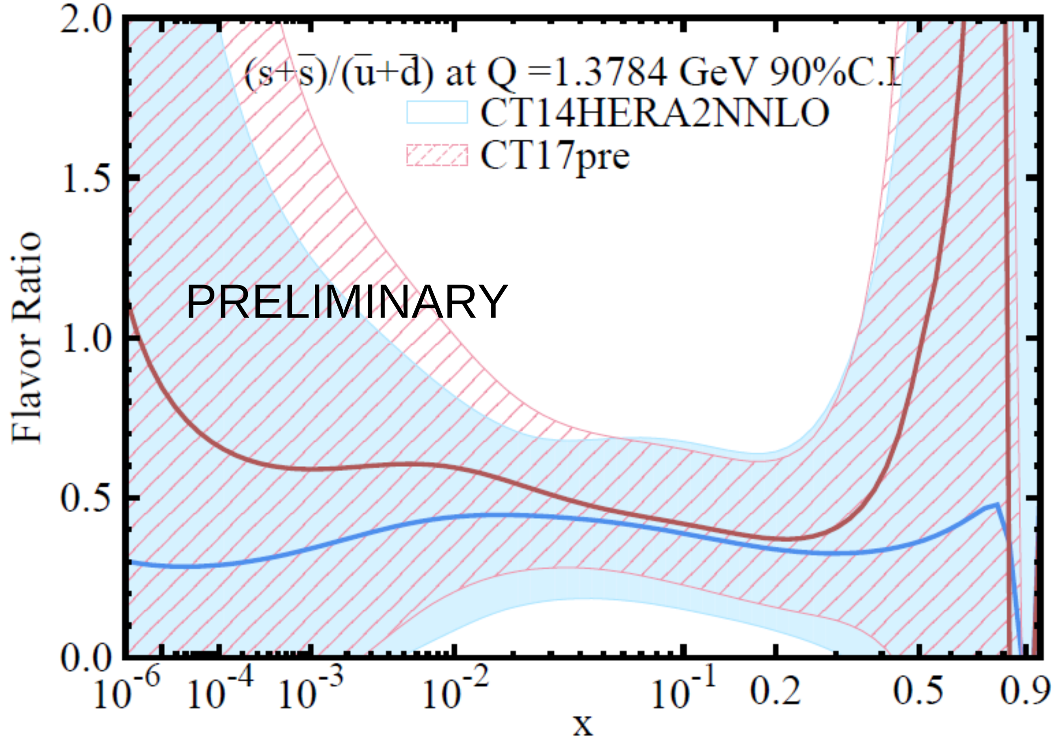

Mild upward pool on $s(x,Q)$ compared to CT14 HERA2

Small to no reduction on the PDF error on $s(x,Q)$

$$R_s(CT17pre) = \frac{s+\bar{s}}{\bar{u}+\bar{d}} = 0.53 \pm 0.16 \text{ (90\% c.l.) at } x = 0.023,\ Q^2 = 1.9\ \mathrm{GeV}^2$$

Effect of LHC data on strangeness: the actual CT17pre fit

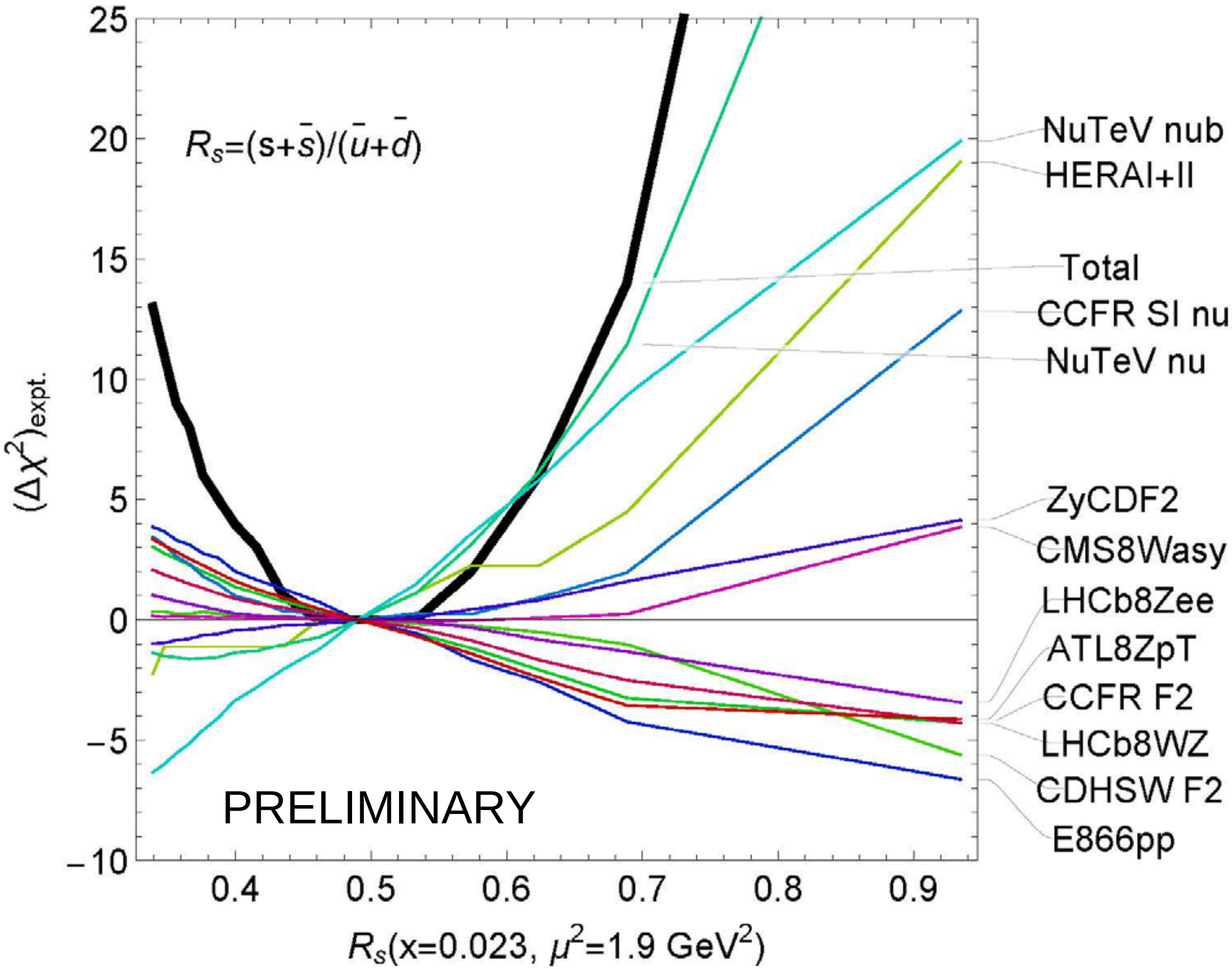

Some tension between NuTeV, CCFR dimuon production, HERAI+II (preferring $R_s < 0.6$);

and vector boson production at the LHC and Tevatron (preferring $R_s > 0.6$)

However, still large uncertainties

Is leading-power NNLO QCD theory sufficient for describing the CTEQ global data?

Can the higher-order/higher-twist corrections survive…

1. … at small x in HERA DIS (“BFKL”; **CT14HERA2**)?

2. … for subleading flavor combinations (“intrinsic charm”; **CT14IC**)?

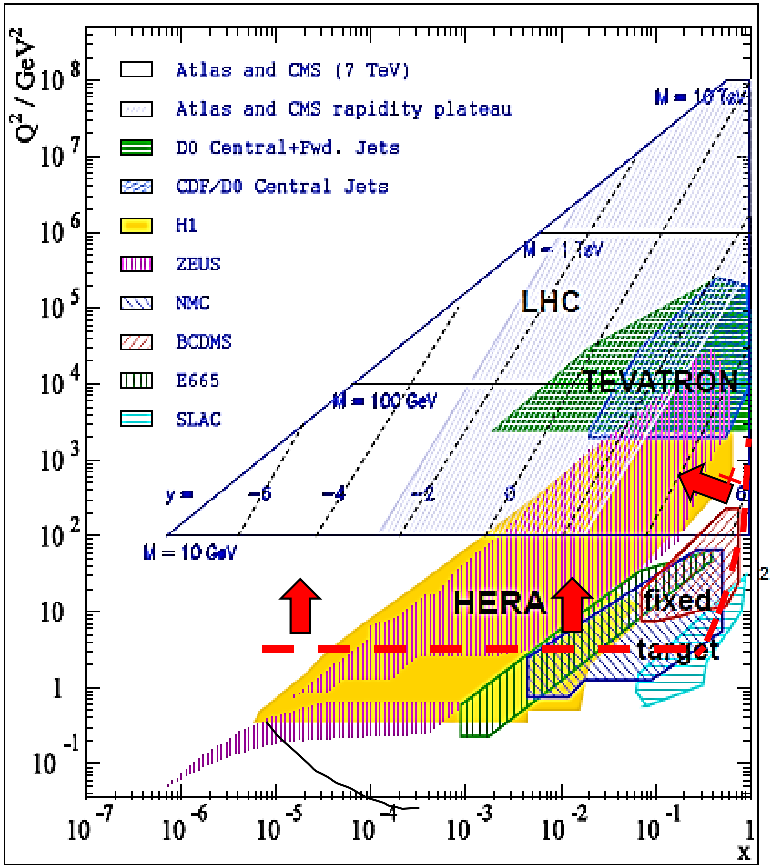

CT14:

only DIS data above the red line with $Q > 2$ GeV, $W > 3.5$ GeV are accepted to ensure stable NNLO predictions

Some higher-order corrections may survive in parts of phase space

CT14 PDFs with HERA1+2 (=HERA2) combination

Phys.Rev. D95 (2017) 034003

Separate the four HERA2 DIS processes;
(Q_{cut} = 2 GeV)

	N_{pts}	$\chi^2_{red.} / N_{pts}$
NC e^+p	880	1.11
CC e^+p	39	1.10
NC e^-p	159	1.45
CC e^-p	42	1.52
totals		
[reduced χ^2] /N	1120	1.17
χ^2 / N	1120	1.25
R^2 / N	1120	0.08

e^+p data are fitted fine

e^-p data are fitted poorly

reduced χ^2 values

χ^2 = [reduced χ^2] + R^2

The quadratic penalty for 162 systematic errors = 87.5

CT14 PDFs with HERA1+2 (=HERA2) data

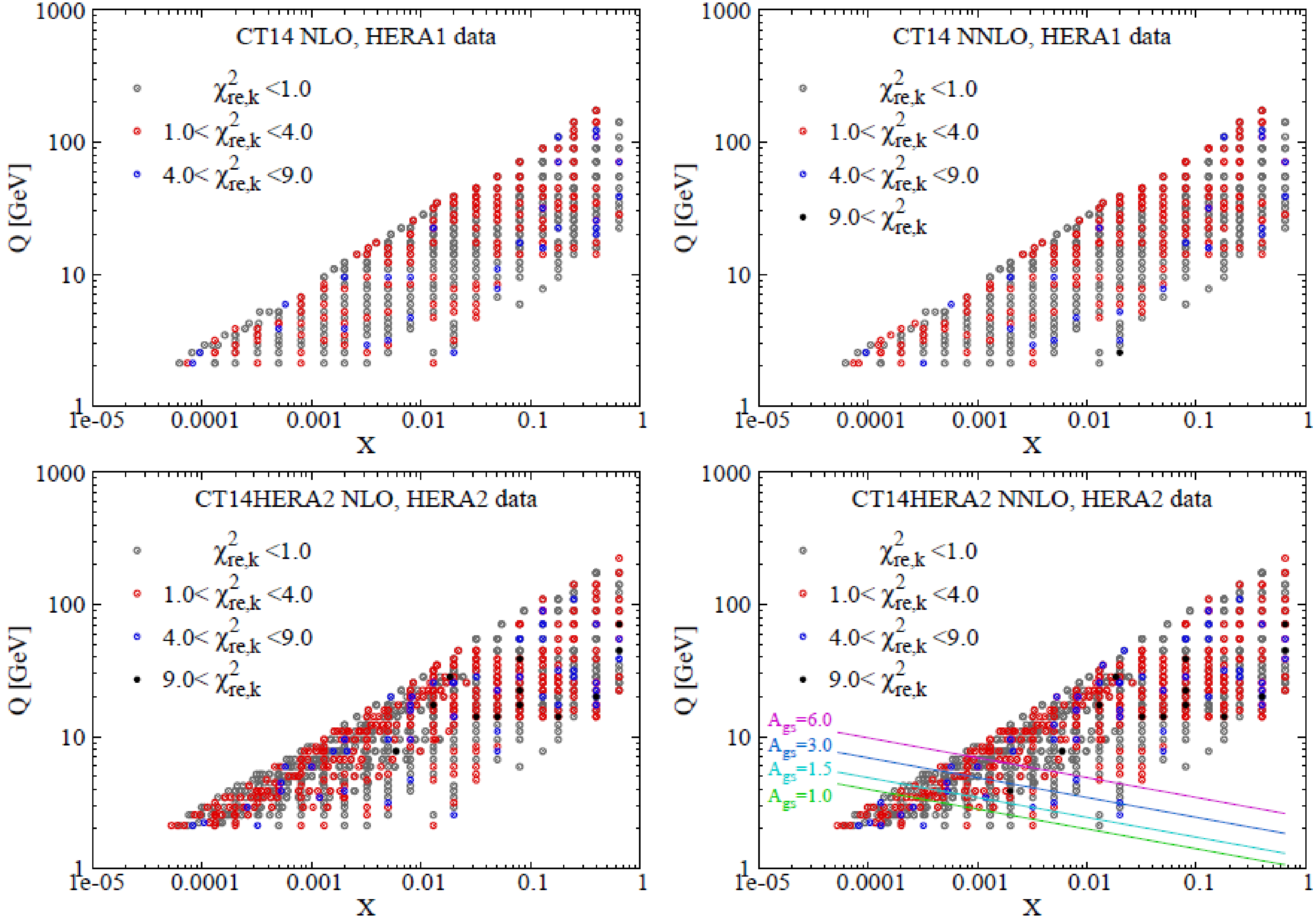

Points with excessive χ^2 are randomly scattered in the $\{x, Q\}$ plane

Stability of CT14 HERA2 fit

- The fit quality does not change much when we vary lower cuts on Q and $A_{gs} = x^{0.3}Q^2$, or increase statistical weight of the HERA2 data

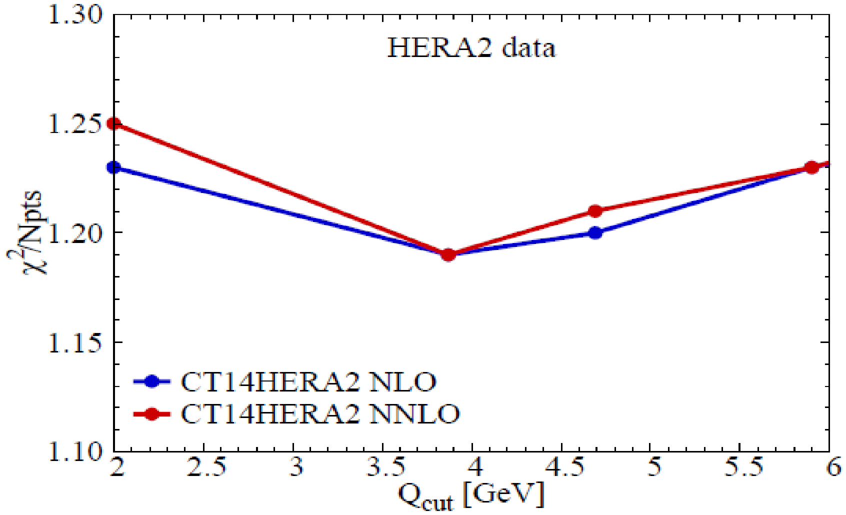

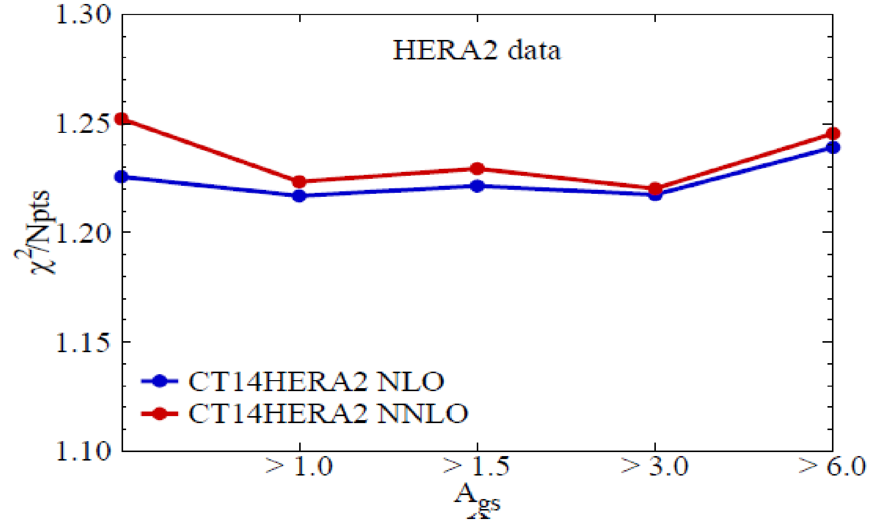

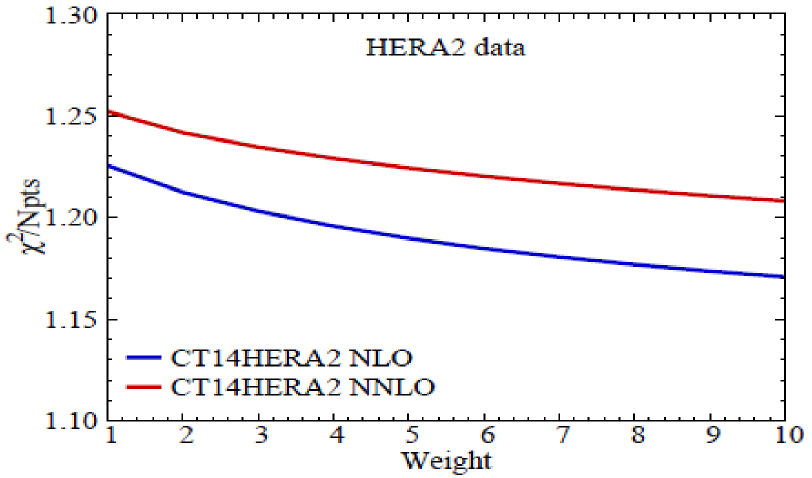

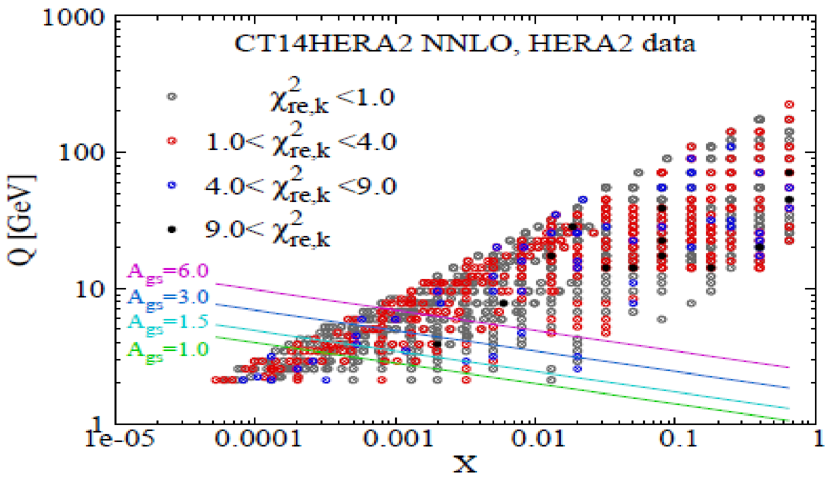

CT14HERA2 vs. CT14 PDFs: central sets

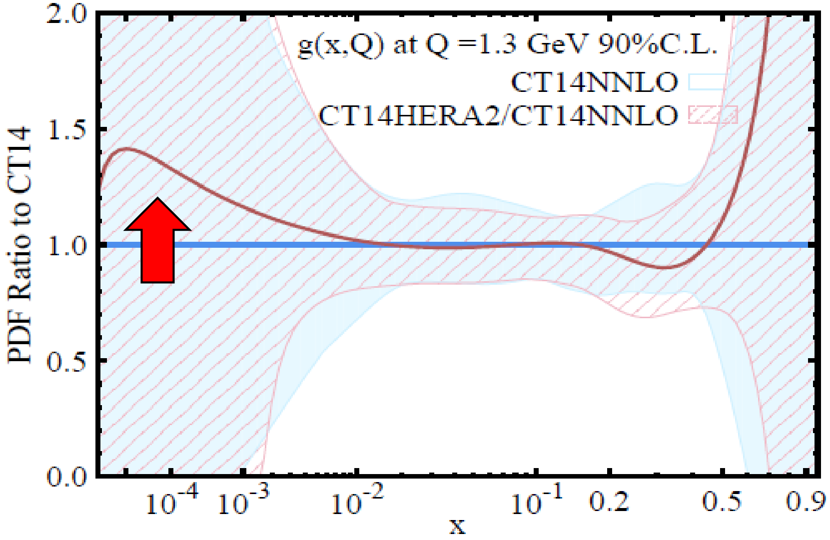

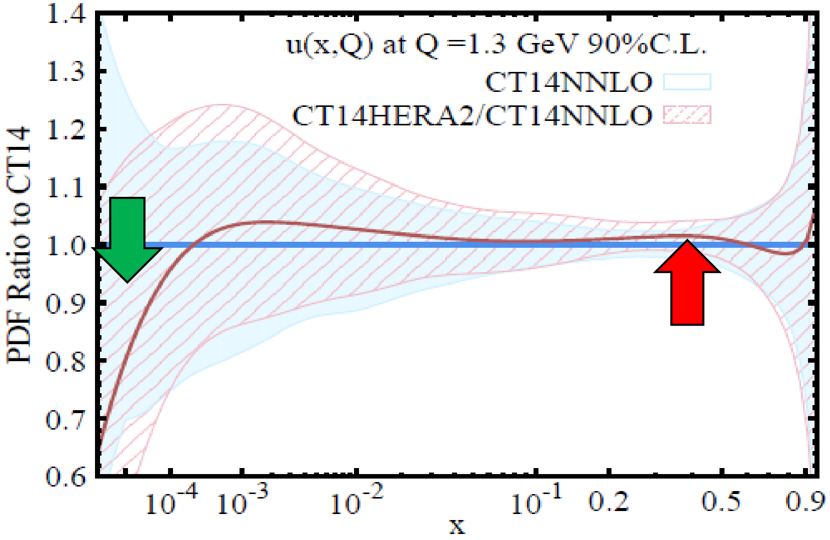

All changes are within CT14 uncertainties

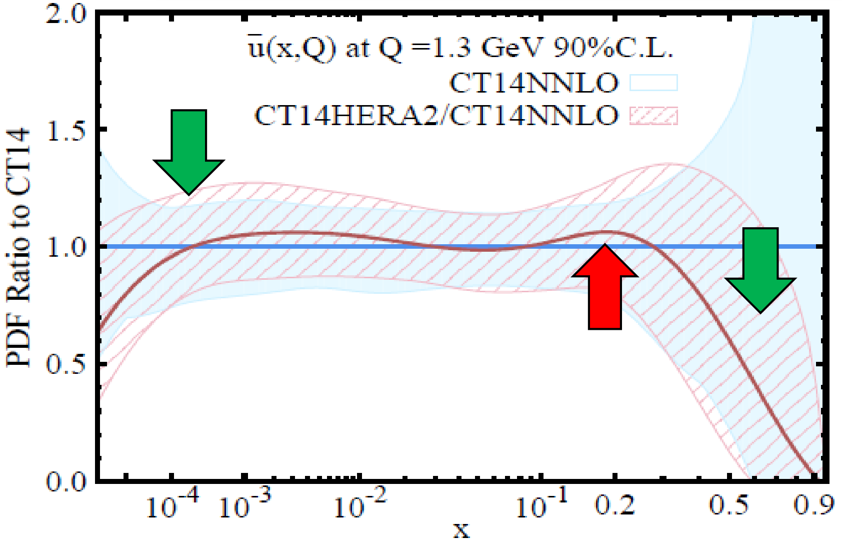

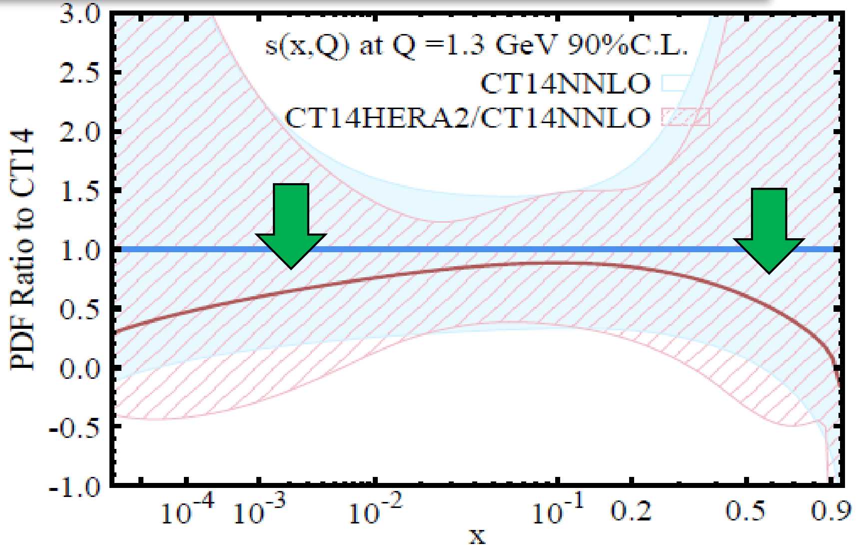

CT14HERA2 PDFs at small x

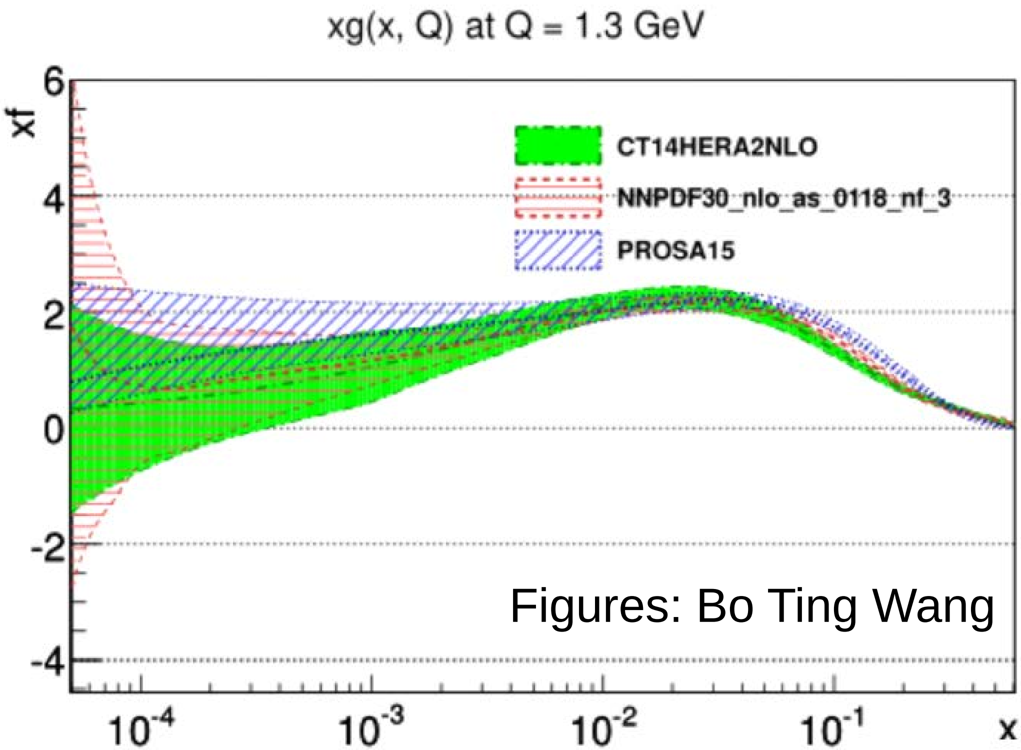

Figures: Bo Ting Wang

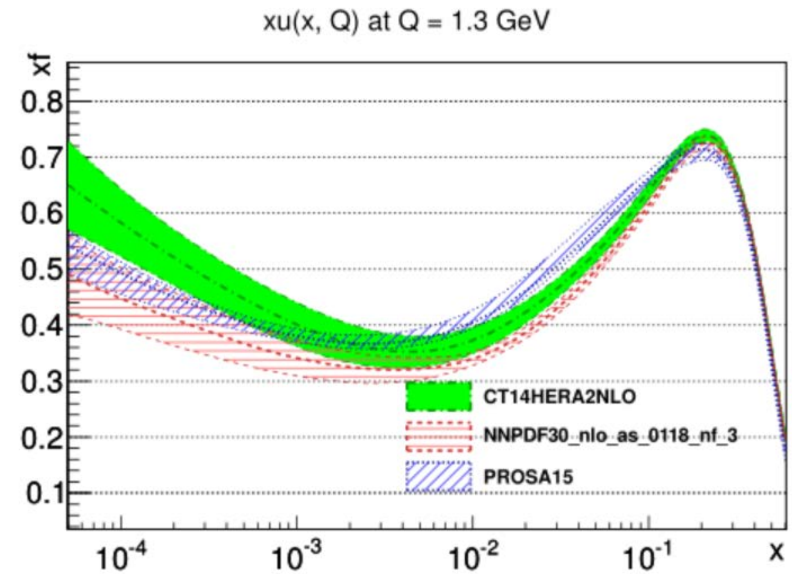

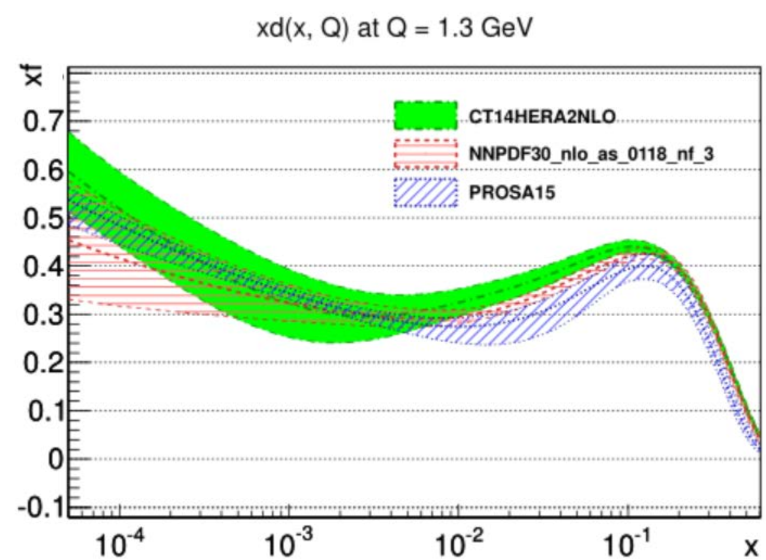

At $x < 10^{-2}$, the CT14HERA2 NLO $N_f = 3$ gluon is compatible with PROSA'15 PDFs fitted to 7 TeV LHCb heavy-flavor production data. Next rounds of LHCb measurements may help constrain the small-x gluon.

A twist-4 contribution in HERA DIS charm production ($\subset$ "intrinsic charm")

[arXiv:1707.00065]

Twist-2
$\gamma^* g \to c\bar{c}$

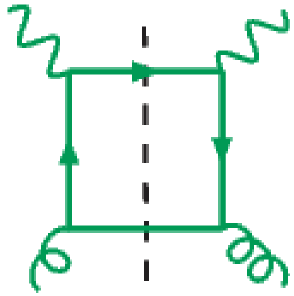

Order $\alpha_s(Q)$

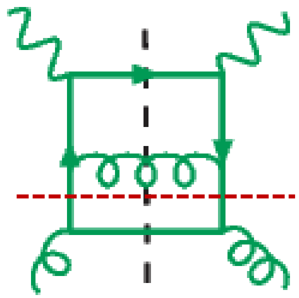

$\alpha_s^2(Q) \cdot \ln(Q^2/m_c^2)$

A ladder; must be resummed in $c(x, Q)$ in the $N_f = 4$ scheme at $Q^2 \gg m_c^2$; e.g., in the ACOT scheme

Twist-4
$\gamma^*(gg) \to c\bar{c}$

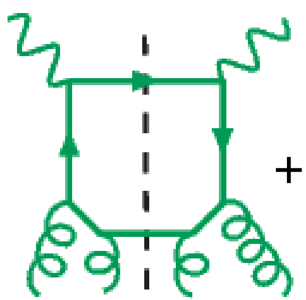

+…

$\Lambda \lesssim 1$ GeV

$\alpha_s^2(Q) \cdot (\Lambda^2/Q^2)$
or $\alpha_s^2(Q) \cdot (\Lambda^2/m_c^2)$

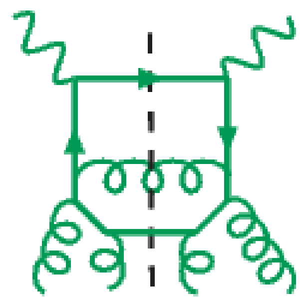

$\alpha_s^3(Q) \cdot (\Lambda^2/m_c^2)\,\ln(Q^2/m_c^2)$

A twist-4 contribution in HERA DIS charm production (⊂ "intrinsic charm")

[arXiv:1707.00065]

Twist-2
$\gamma^* g \to c\bar{c}$

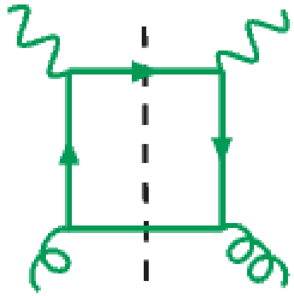

Order $\alpha_s(Q)$

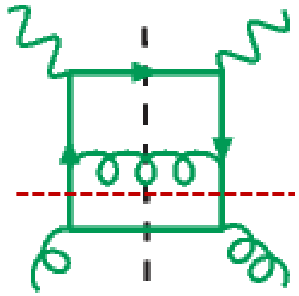

$\alpha_s^2(Q) \cdot \ln(Q^2/m_c^2)$

A ladder; must be resummed in $c(x,Q)$ in the $N_f = 4$ scheme at $Q^2 \gg m_c^2$; e.g., in the ACOT scheme

Twist-4
$\gamma^*(gg) \to c\bar{c}$

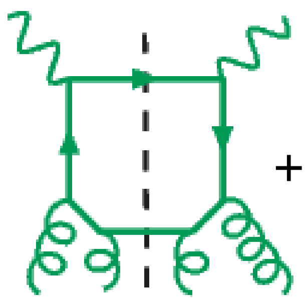

+…

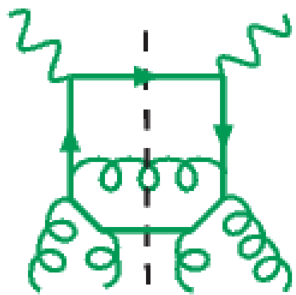

$\Lambda \lesssim 1$ GeV

$\alpha_s^2(Q) \cdot (\Lambda^2/Q^2)$
or $\alpha_s^2(Q) \cdot (\Lambda^2/m_c^2)$

$\alpha_s^3(Q) \cdot (\Lambda^2/m_c^2)\ln(Q^2/m_c^2)$

Can be of order ~10% of the twist-2 α_s^2 term

A twist-4 contribution in HERA DIS charm production ($\subset$ “intrinsic charm”)

[arXiv:1707.00065]

Twist-2
$\gamma^* g \to c\bar{c}$

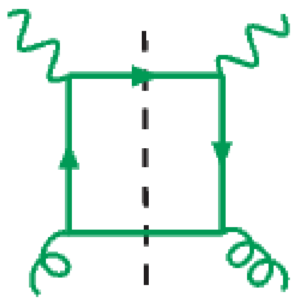

Order $\alpha_s(Q)$

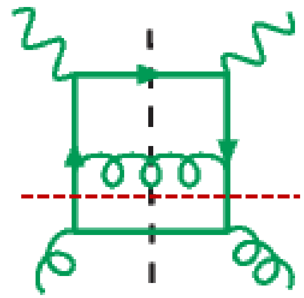

$\alpha_s^2(Q) \cdot \ln(Q^2/m_c^2)$

A ladder; must be resummed in $c(x,Q)$ in the $N_f = 4$ scheme at $Q^2 \gg m_c^2$; e.g., in the ACOT scheme

Twist-4
$\gamma^*(gg) \to c\bar{c}$

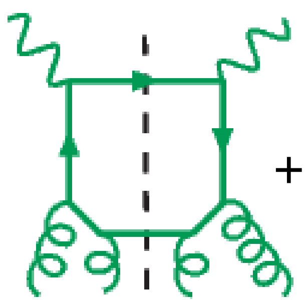

+…

$\Lambda \lesssim 1$ GeV

$\alpha_s^2(Q) \cdot (\Lambda^2/Q^2)$
or $\alpha_s^2(Q) \cdot (\Lambda^2/m_c^2)$

Can be of order ~10% of the twist-2 α_s^2 term

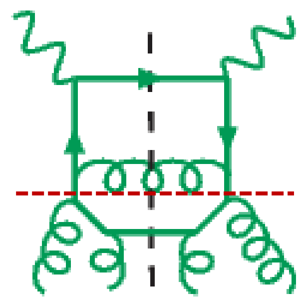

$\alpha_s^3(Q) \cdot (\Lambda^2/m_c^2) \ln(Q^2/m_c^2)$

The ladder subgraphs can be resummed as a part of $c(x,Q)$ in the $N_f = 4$ scheme at $Q^2 \gg m_c^2 > \Lambda^2$;

contribute to the boundary condition for $c(x, Q_0)$ at $Q_0 \approx m_c$;

obey twist-2 DGLAP equations.

CT14 IC study clarifies important questions

What are phenomenological constraints on the "intrinsic charm" from the global QCD data?

⇒ The CT14 charm PDFs allow a "nonperturbative" component carrying a total momentum fraction $\langle x_{IC} \rangle = 1 - 2\%$ in DIS at $Q \approx m_c$.

Can we estimate its impact on the LHC predictions?

Yes, based on the simplest approximation of the "nonperturbative" charm contribution. In most cases, the estimated impact is less than the net CT14 PDF uncertainty.

Twist-4
$\gamma^*(gg) \rightarrow c\bar{c}$

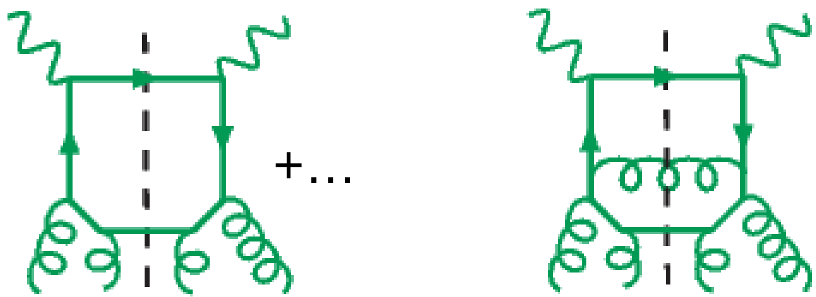

$\alpha_s^2(Q) \cdot (\Lambda^2/Q^2)$
or $\alpha_s^2(Q) \cdot (\Lambda^2/m_c^2)$

$\alpha_s^3(Q) \cdot (\Lambda^2/m_c^2) \ln(Q^2/m_c^2)$

[arXiv:1707.00065]

Note:
"intrinsic charm" ≠ "fitted charm"

PDF fits may include a ``fitted charm'' PDF

``Fitted charm'' = ``higher-twist charm''

+ other (possibly not universal)

higher O(α_s) / higher power terms

QCD factorization theorem for DIS structure function $F(x,Q)$ [Collins, 1998]:

All α_s orders:

$$F(x,Q) = \sum_{a=0}^{N_f} \int_x^1 \frac{d\xi}{\xi} \mathcal{C}_a\left(\frac{x}{\xi}, \frac{Q}{\mu}, \frac{m_c}{\mu}; \alpha(\mu)\right) f_{a/p}(\xi,\mu) + \mathcal{O}(\Lambda^2/m_c^2, \Lambda^2/Q^2).$$

The PDF fits implement this formula up to (N)NLO (N_{ord} = 1 or 2):

PDF fits:

$$F(x,Q) = \sum_{a=0}^{N_f} \int_x^1 \frac{d\xi}{\xi} \mathcal{C}_a^{(N_{ord})}\left(\frac{x}{\xi}, \frac{Q}{\mu}, \frac{m_c}{\mu}; \alpha(\mu)\right) f_{a/p}^{(N_{ord})}(\xi,\mu).$$

The perturbative charm PDF component cancels at $Q \approx m_c$ up to a higher order

The 'fitted charm component' may approximate for missing terms of orders α_s^p with $p > N_{ord}$, or Λ^2/m_c^2, or Λ^2/Q^2 -- generally process-dependent

Dependence on the switching scale (no IC)

If the "fitted charm" is purely twist-2, we expect its effect to vanish for a sufficiently high α_s order of the calculation.

This is analogous to the reduction in the dependence on the switching scale μ_c from 3FS to 4FS, when the α_s order increases for a fixed Q_0 and m_c, as demonstrated recently by the xFitter group

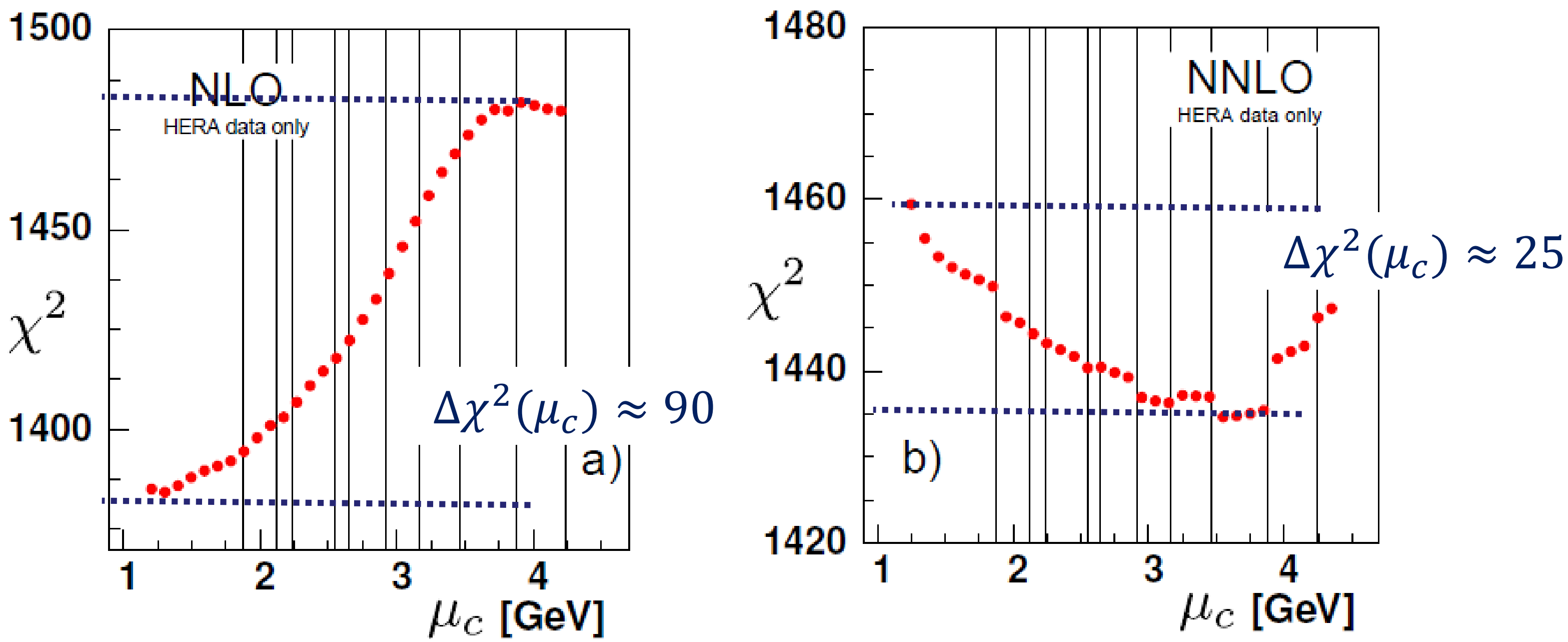

Fig. 5 χ^2 vs. the charm matching scale μ_c at a) NLO and b) NNLO for all data sets. The bin boundaries for the HERA data set "HERA1+2 NCep 920" are indicated by the vertical lines.

Bertone et al. (xFitter), arXiv:1707.05343

Dependence of $\Delta\chi^2$ on the IC momentum fraction $\langle x\rangle_{IC}$

In contrast, a twist-4 "IC" contribution will not decrease when going from N^kLO to $N^{k+1}LO$.

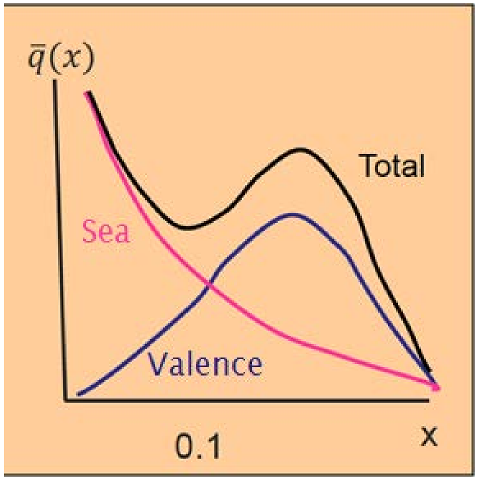

Depending on its dynamical origin, the IC charm takes a variety of shapes, e.g., a "sea-like" (SEA) or "valence-like" form. The Brodsky-Hoyer-Peterson-Sakai form (BHPS) predicts a "valence-like" $c(x, Q_0)$ peaked at $x \sim 0.2$. A sea-like form is monotonic in x.

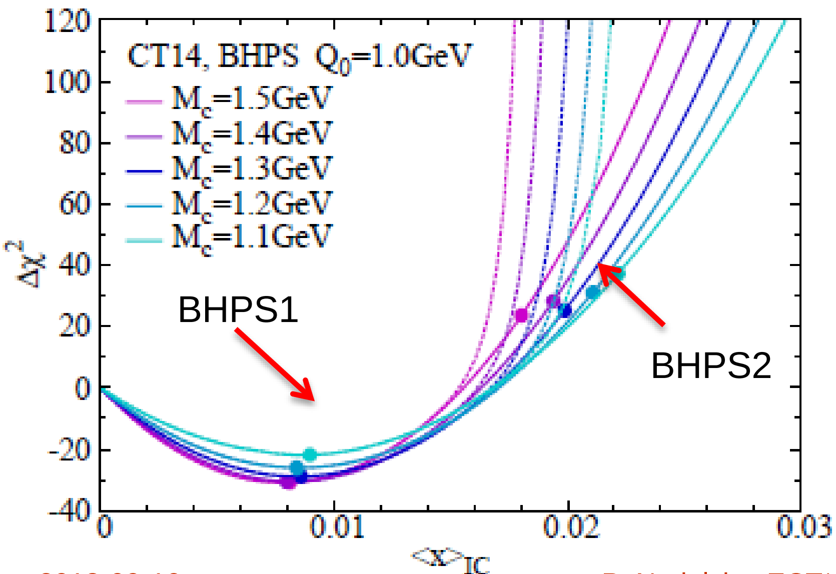

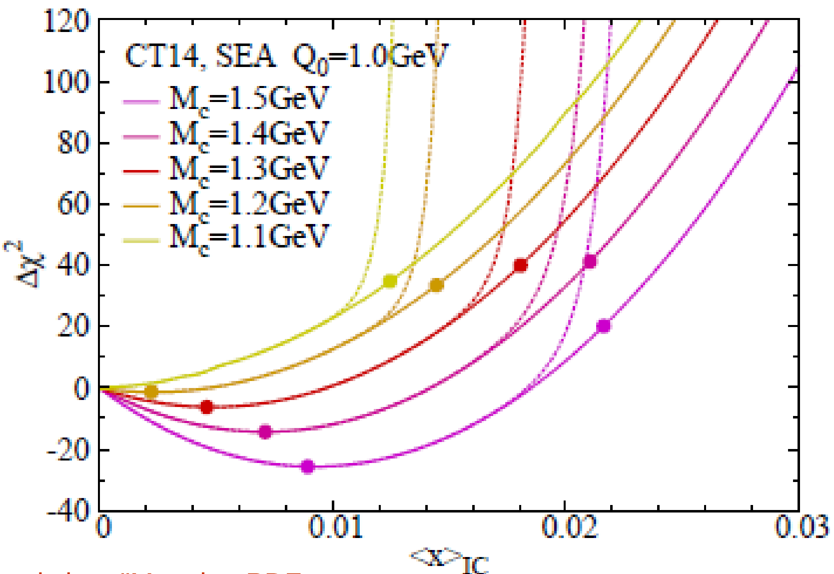

ACOT-like factorization for twist-4 charm contributions (an example)

α_s^2 :

α_s^3 :

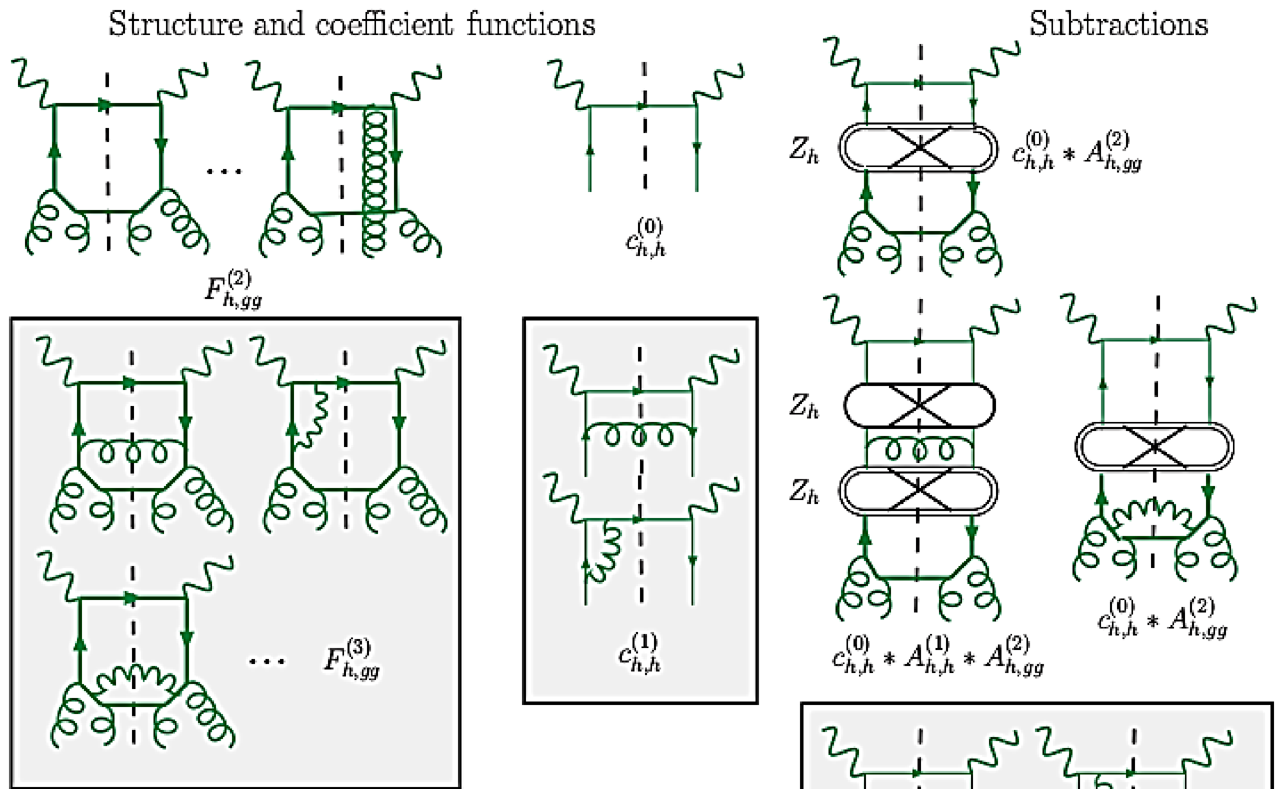

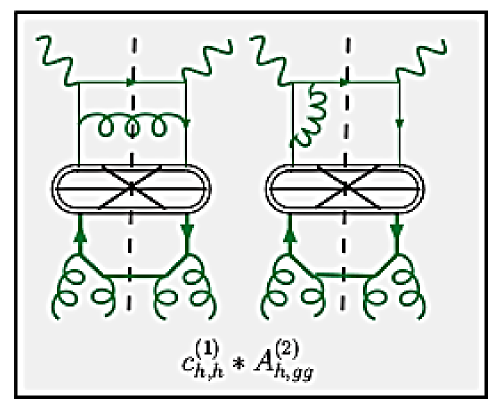

The IC terms can be factorized in the ACOT method into

- universal twist-4 nonperturbative functions $f_{gg}(\xi_1, \xi_2, Q)$, etc.

- process-dependent coefficient functions $c^{(k)}_{h,h}, C^{(k)}_{h,gg}$, etc.

Allowed $c + \bar{c}$ momentum fractions

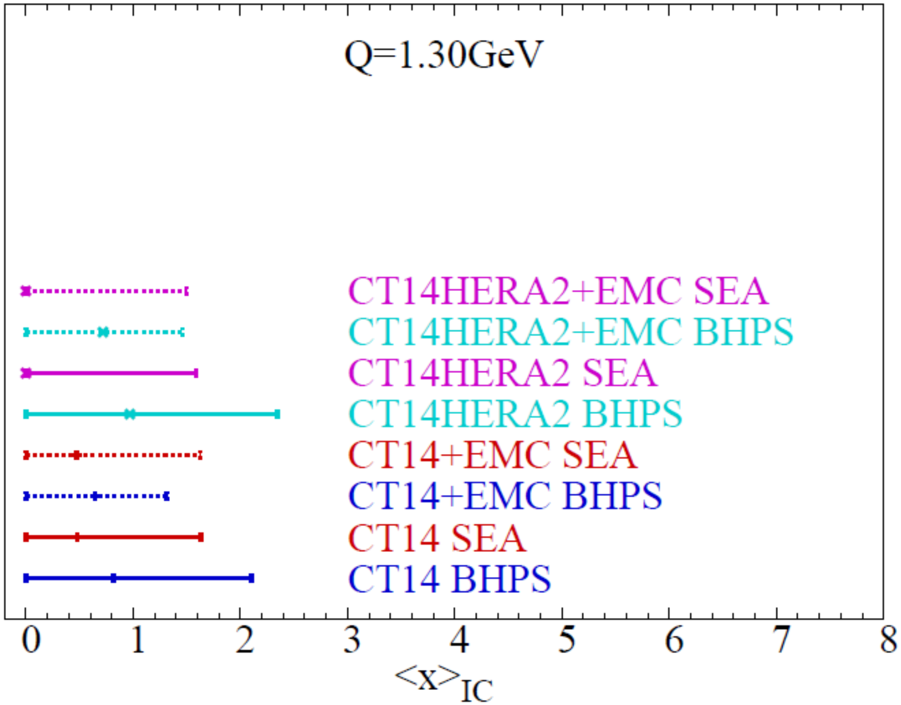

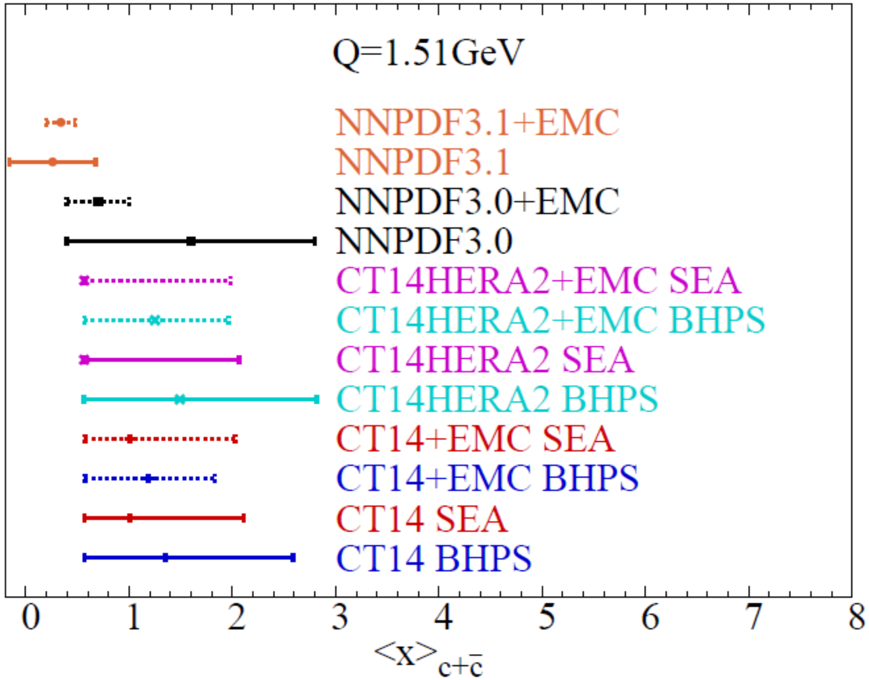

Sources of differences	CT14 IC	NNPDF3.x
α_s order	NNLO only	NLO, NNLO
Settings	90% c.l. from Lagrange multiplier scan $Q_0 = m_c^{pole} = 1.3$ GeV	Symmetric. 68% c.l. from Monte-Carlo sampling, $Q_0 = m_c^{pole} =$ 1.51 GeV
LHC 8 TeV W, Z	Under validation; mild tension with HERA DIS data	Included; strong effect despite a smallish data sample
1983 EMC F_{2c} data included?	Only as a cross check (unknown syst. effects in EMC data)	Optional, strong effect on the PDF error

Impact of IC on the PDF ratios

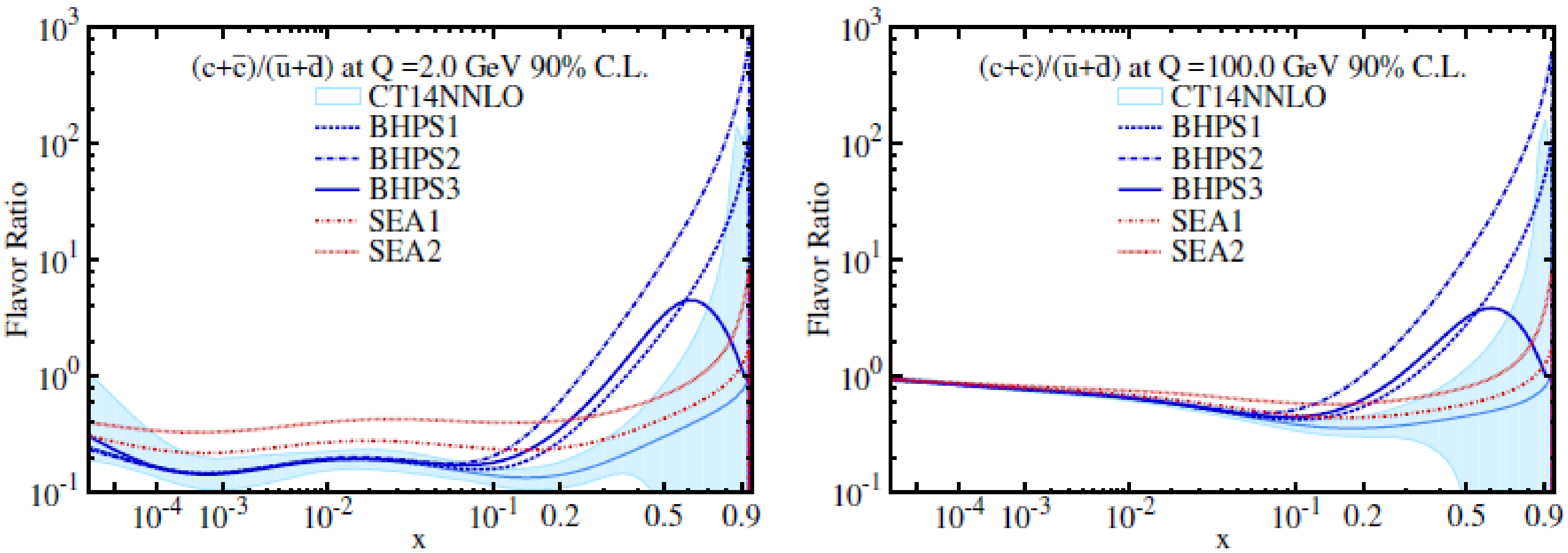

Common parametrizations of the IC may produce an unphysically large ratio $\left(c(x,Q)+\bar{c}(x,Q)\right)/\left(\bar{u}(x,Q)+\bar{d}(x,Q)\right)$ at $x\rightarrow 1$ and low $Q\sim m_c$. This is resolved in the BHPS3 parametrization, which solves the BHPS model numerically and introduces small valence-like components in $\bar{u}(x,Q_0)$ and $\bar{d}(x,Q_0)$ to moderate their drop at $x\rightarrow 1$.

Outlook for CTEQ-TEA PDFs

- **Ongoing CTEQ-TEA PDF analysis**

Detailed investigation of the LHC 7 and 8 TeV vector boson, jet, $t\bar{t}$ production data suggests mild changes in the central fits, PDF uncertainties, and precision EW observables, as compared to the CT14HERA2 NNLO data set. We notice the potential of the future ATLAS/CMS jet data, together with other LHC processes, for strengthening the constraints on the g, s, $\bar{u}$, and $\bar{d}$ PDFs with modest improvements in experimental systematics and full implementation of NNLO jet cross sections

- **CT14 PDFs** with photon PDFs **[1509.02905]**, intrinsic/fitted charm **[1706.00657]**, and Monte-Carlo error PDFs **[1607.06066]**
- NLO calculation for ***c*, *b* production at LHCb, ATLAS** in the S-ACOT-χ
- scheme using MCFM/Applgrid **[Campbell, P. N., Xie, in pre-publication]**
- Further development of programs for fast survey **[PDFSense]** and Hessian reweighting of the data **[ePump]**

Oekumene of the PDF universe

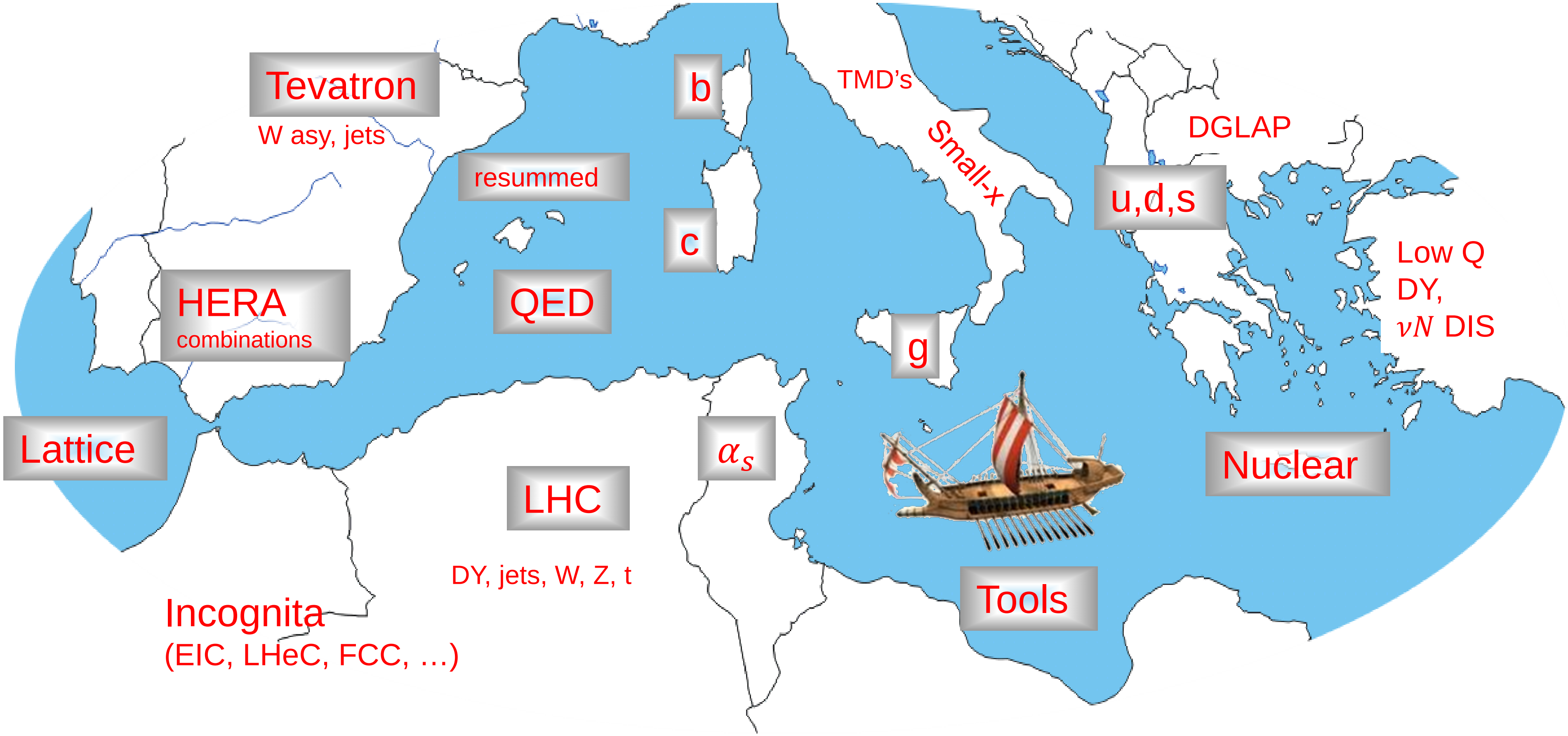

New lands for charting,
new tools for exploring

Workshop on Parton distributions as a bridge from low to high energies

November 8 and 9, 2018

[before the CTEQ meeting]

Jefferson Laboratory, Newport News, VA

- **Multi-dimensional PDFs (TMDs and GPDs)**
- **Collinear parton distributions at JLab 12, EIC, and LHeC**
- **QCD and Nuclear PDFs in electron-nucleus and neutrino-nucleus scattering**

Jefferson Lab
Thomas Jefferson National Accelerator Facility

C T E Q

Extra details

CT14: parametrization forms

- CT14 relaxes restrictions on several PDF combinations that were enforced in CT10. [These combinations were not constrained by the pre-LHC data.]
  - The assumptions $\frac{\bar{d}(x,Q_0)}{\bar{u}(x,Q_0)} \to 1$, $u_v(x,Q_0) \sim d_v(x,Q_0) \propto x^{A_{1v}}$ with $A_{1v} \approx -\frac{1}{2}$ at $x < 10^{-3}$ are relaxed once LHC W/Z data are included
  - CT14 parametrization for $s(x,Q)$ includes extra parameters
- Candidate CT14 fits have 30-35 free parameters
- In general, $\mathrm{f_a}\,(\mathrm{x}, \mathrm{Q_0}) = \mathrm{A}x^{a_1}(1-\mathrm{x})^{\mathrm{a_2}}\mathrm{P_a}(\mathrm{x})$
- CT10 assumed $P_a(x) = \exp(a_0 + a_3\sqrt{x} + a_4 x + a_5\, x^2)$
  - exponential form conveniently enforces positive definite behavior
  - but power law behaviors from a_1 and a_2 may not dominate
- In CT14, $\mathrm{P_a}(\mathrm{x}) = \mathrm{G_a}(\mathrm{x})\mathrm{F_a}(\mathrm{z})$, where $\mathrm{G_a}(\mathrm{x})$ is a smooth factor
  - $\mathrm{z} = 1 - 1(1-\sqrt{\mathrm{x}})^{\mathrm{a_3}}$ preserves desired Regge-like behavior at low x and high x (with $\mathrm{a_3}$>0)
- Express $F_a(z)$ as a linear combination of Bernstein polynomials:

$$z^4, 4z^3(1-z), 6z^2(1-z)^2\,, 4z(1-z)^3, (1-z)^4$$

  - each basis polynomial has a single peak, with peaks at different values of z; reduces correlations among parameters

(N+1)-dim. perspective eliminates wrong N-dim. solutions

Hessian error PDFs (CT10)

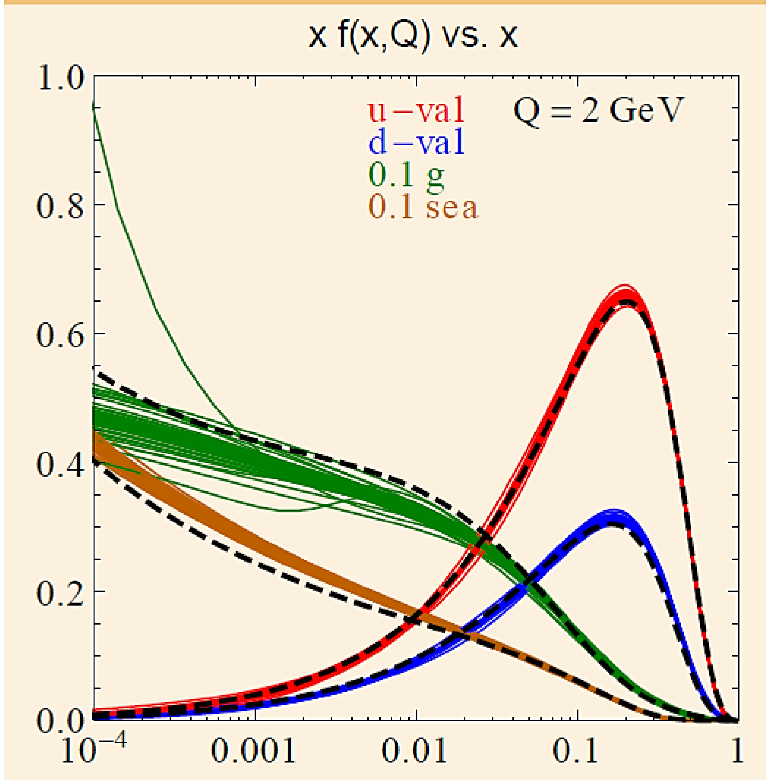

Neural network PDFs

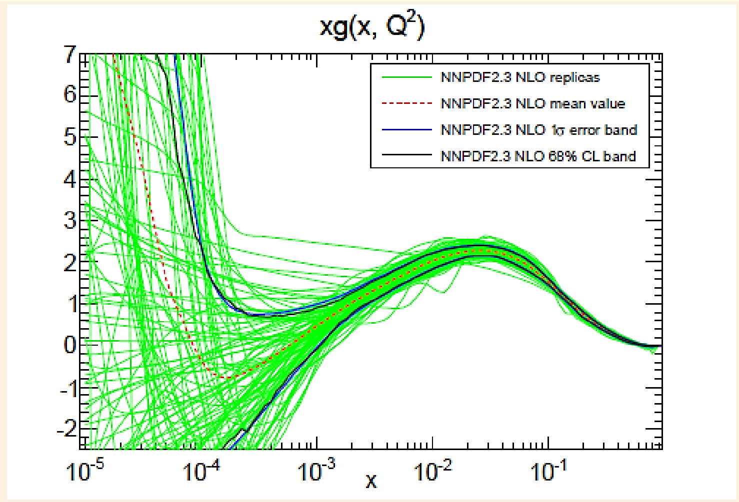

CJ15: DIS data for $Q^2 > 1.3\ GeV^2$, $W^2 > 3\ GeV^2$

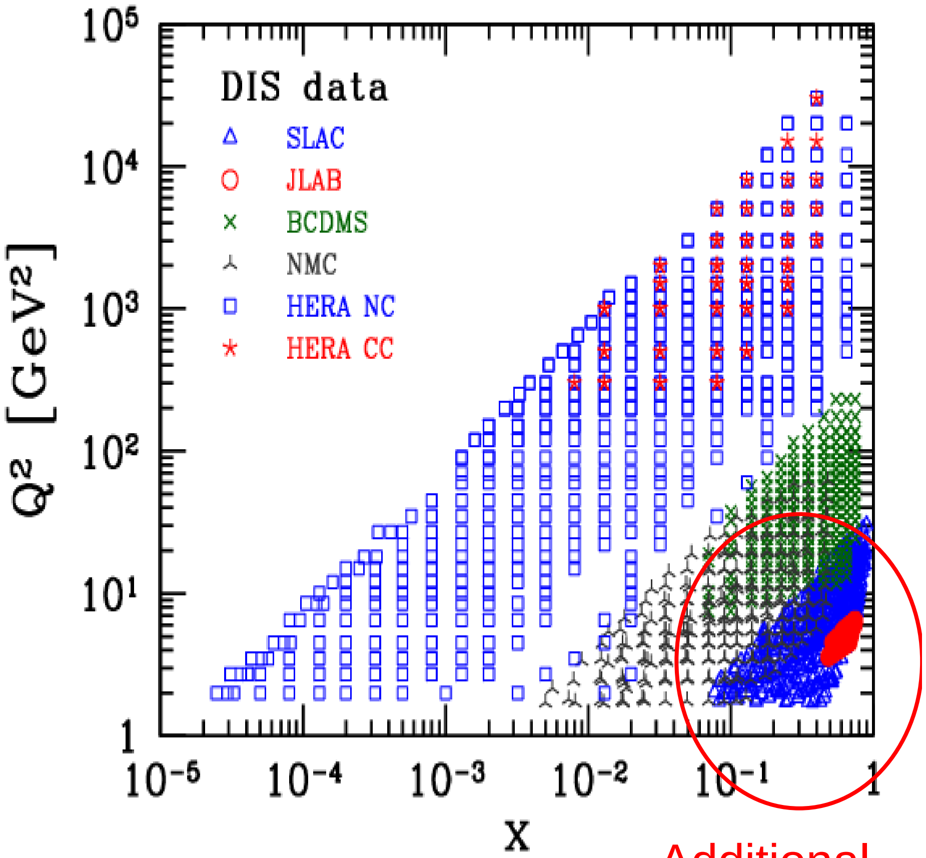

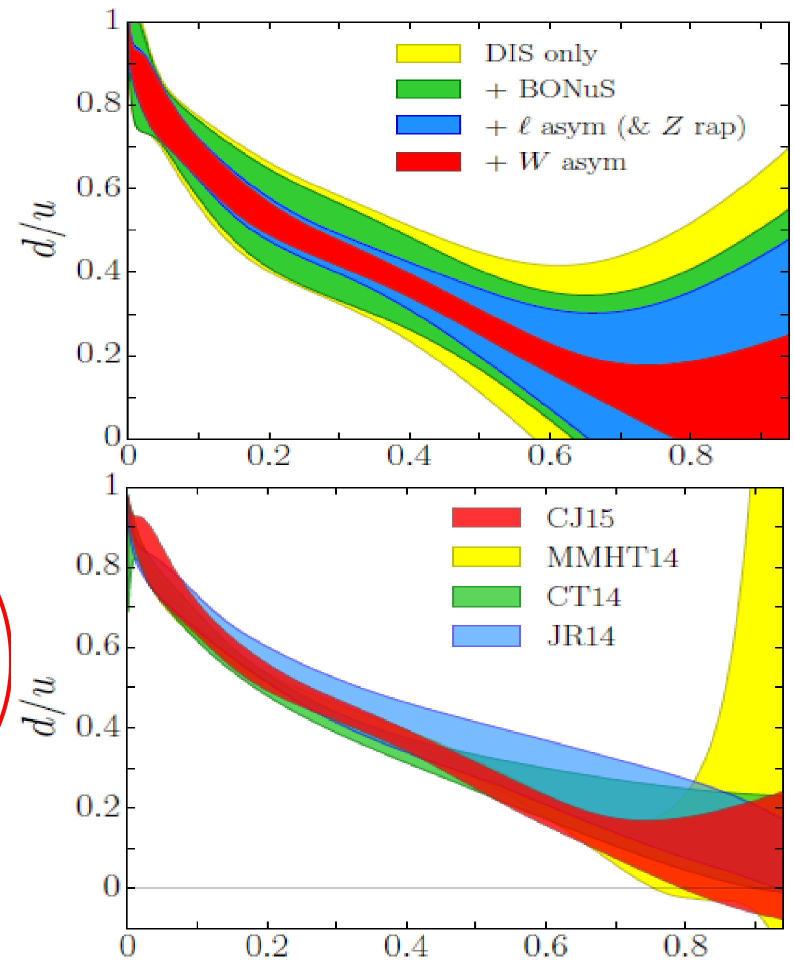

FIG. 16: Comparison of the d/u ratio at $Q^2 = 10$ GeV^2 for different PDF parametrizations: CJ15 (red band), MMHT14 [6] (yellow band), CT14 [7] (green band), and JR14 [10] (blue band).

Flavor composition of PDFs

SU(2) and charge symmetry breaking

$\bar{d}(x) \neq \bar{u}(x), q(x) \neq \bar{q}(x)$

May be caused by

- DGLAP evolution
- Fermi motion
- Electromagnetic effects
- Nonperturbative meson fluctuations
- Chiral symmetry breaking
- Instantons
- …

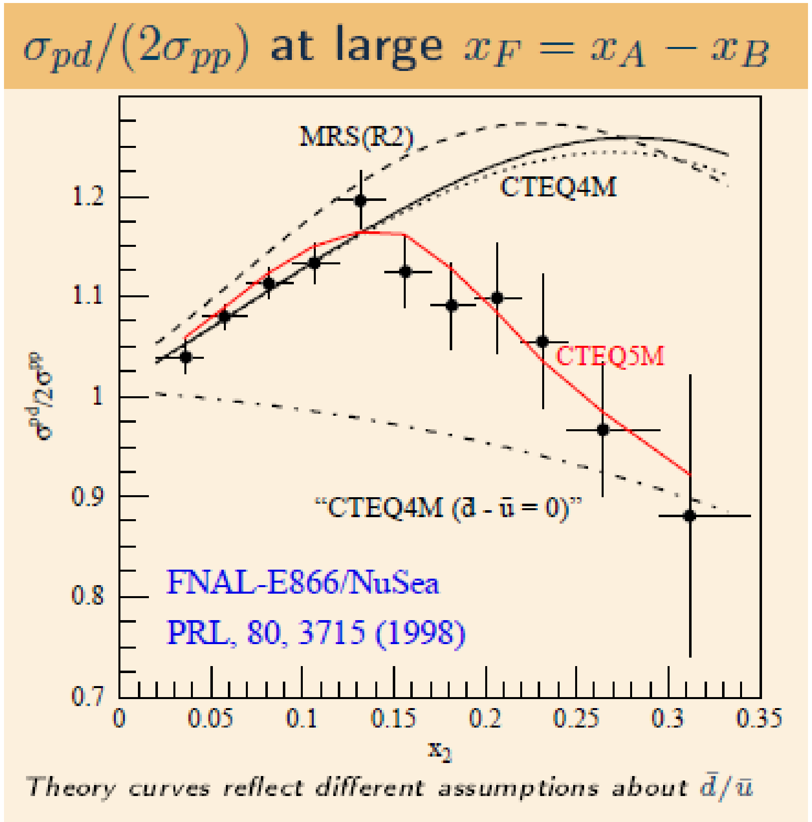

Extrinsic and intrinsic sea PDFs

$(\bar{q} = \bar{u}, \bar{d}, \bar{s}, \bar{c}, \bar{b})$

"Extrinsic" sea
(maps on disconnected diagrams of lattice QCD for both heavy and light flavors?)

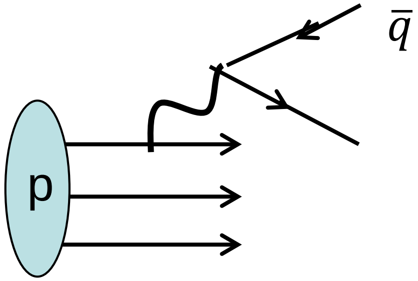

"Intrinsic" sea (excited Fock nonpert. states, maps on connected diagrams of lattice QCD?)

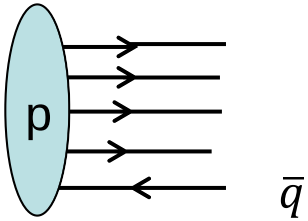

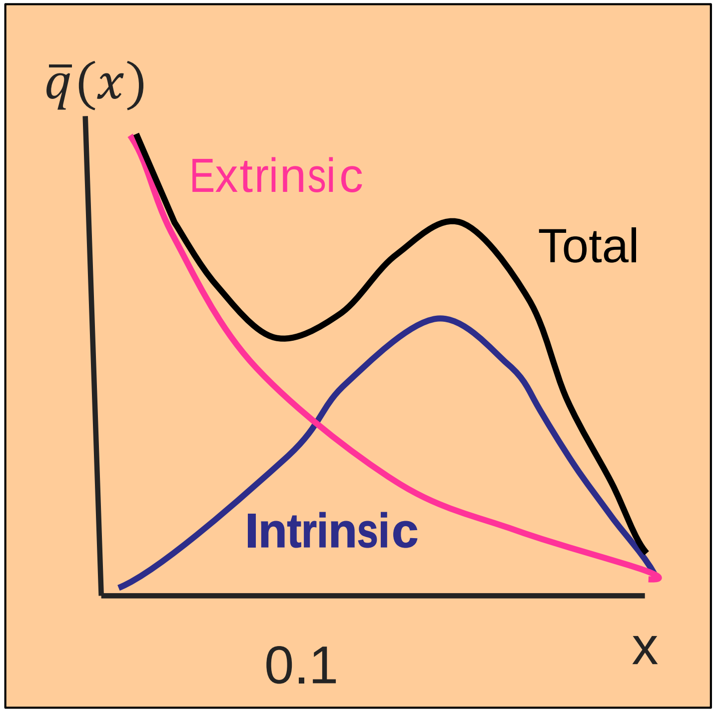

Extrinsic and intrinsic sea PDFs

Smooth $\bar{u} + \overline{d}$ parametrizations can hide existence of two components

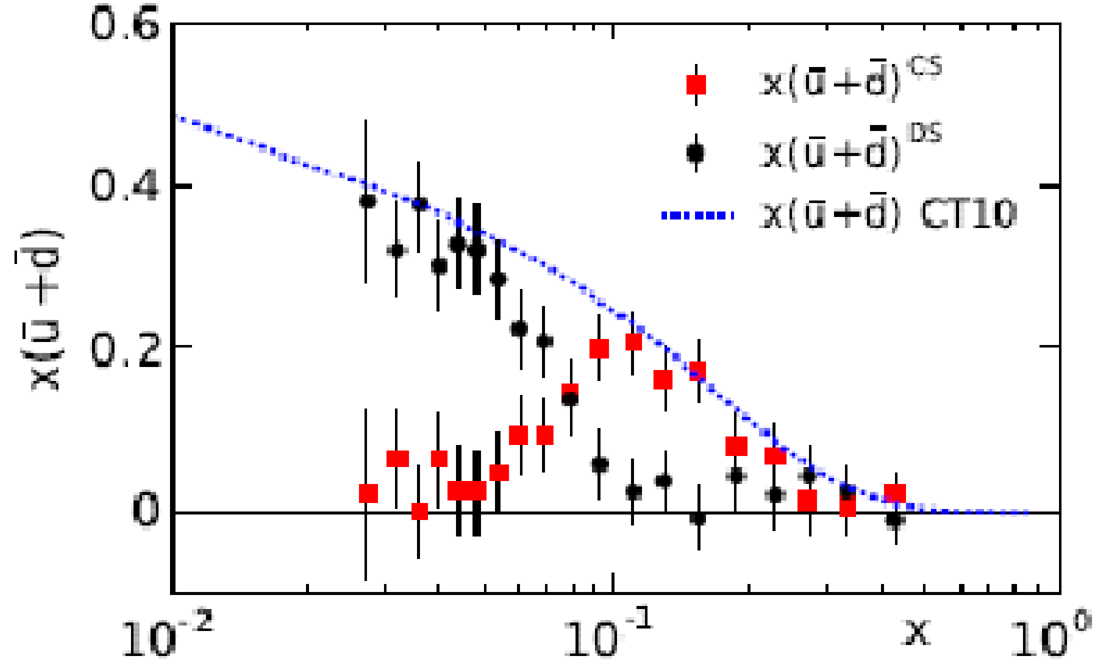

FIG. 5: $x(\bar{u}^{cs}(x)+\bar{d}^{cs}(x))$ obtained from Eq. (1) is plotted together with $x(\bar{u}(x)+\bar{d}(x))$ from CT10 and $\frac{1}{R}x(s(x)+\bar{s}(x))$ which is taken to be $x(\bar{u}^{ds}(x)+\bar{d}^{ds}(x))$.

Liu, Chang, Cheng, Peng, 1206.4339

(Dis)connected topologies in lattice QCD

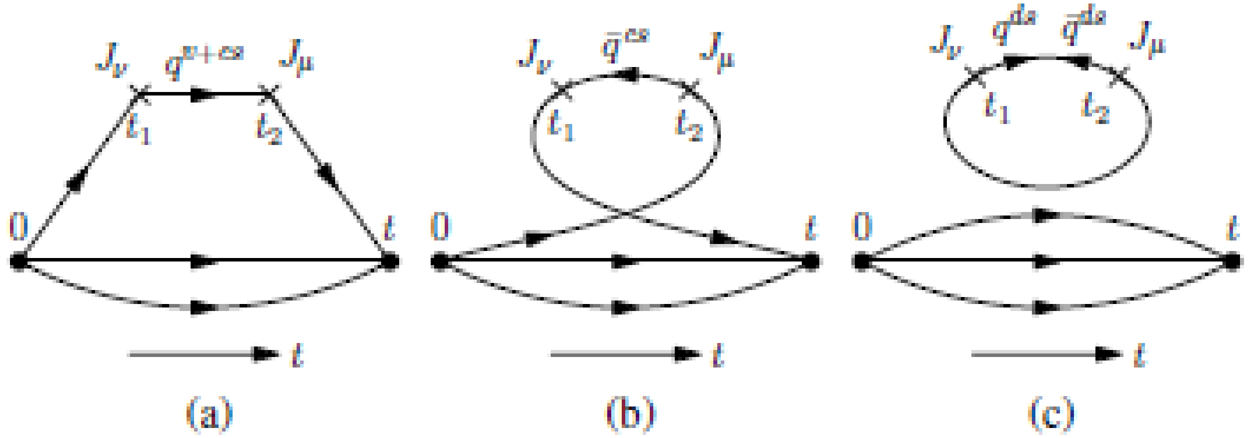

FIG. 1: Three gauge invariant and topologically distinct diagrams in the Euclidean path-integral formalism of the nucleon hadronic tensor in the large momentum frame. In between the currents at t_1 and t_2, the parton degrees of freedom are (a) the valence and CS partons q^{v+cs}, (b) the CS anti-partons $\bar{q}^{cs}$, and (c) the DS partons q^{ds} and anti-partons $\bar{q}^{ds}$ with $q = u, d, s$, and c. Only u and d are present in (a) and (b).

Liu, Chang, Cheng, Peng, 1206.4339